Abstract.

Along history, hydrofoils have accompanied Men in their search for the perfect watercraft that would offer both efficiency and velocity, while assuring the user's security and comfort. Several worldwide celebrated personalities have participated in this endless quest, and have aided hydrofoils to develop their capabilities towards their fully potential. Nevertheless, despite their many advantages, hydrofoils still occupy a secondary role in many sports like windsurfing, and are yet to reach plaid people who seem oblivious to their existence. However, this project states that many windsurfing companies – like AHD – are demonstrating a slow but constant interest in attaching hydrofoils to their boards, thus contributing to an enhancement of hydrofoils market.

Due to their many benefits, hydrofoils have been the object of several studies over the years. This particular project is based on Laura Voltà and Júlia Solanes previous research report: *Hidrodinàmica i Aplicacions dels Hydrofoils al Windsurf*, whose objective was to demonstrate how hydrofoils increase the lift coefficient of a windsurfing board, and allow it to reach higher velocities. Therefore, the current project focused on extending the previous one, providing an optimization of the hydrofoil profile – the Eppler E211 – by designing and attaching a winglet. The addition of the winglet was destined to ameliorate the behavior of the profile in terms of drag reduction.

When travelling through water, hydrofoils cause a gradient of pressure between the upper and the lower section of the profile, which eventually translates into the generation of wingtip vortices similar to those that appear in many aircrafts. Therefore, these lift induced vortices produce *Induced drag*, which can be reduced by, for example, adding winglets to the profile. As it is stated in this project, in the previous research report the E211 presented an induced drag of 0, 0206, which was calculated in order to be able to set the conditions that had to be met so a perceivable reduction of induced drag could be possible.

After generating some winglet geometries with SolidWorks and analyzing them with ANSYS Fluent, the diverse results obtained were compared to the already existing induced drag coefficient, in order to find the best solution. Finally, this project concluded that the blended winglet with bias tip was the one whose results got closer to the desired calculated values; obtaining a substantial increase of the lift coefficient, whose value was now of **0,575** (bigger than the 0,43 original value); and a consequent reduction of drag, whose value was now of **0,0275** (smaller than the 0, 029 original value). Therefore, judging by the results obtained by the blended winglet with bias tip, it is obvious that it had become the best option to optimize the E211 profile. The growth of the lift coefficient occurred due to the fact that a great part of the lift was being used to compensate the destabilizing effect that induced drag had on the hydrofoil. However, once the induced drag had been reduced, the lift coefficient increased because it no longer had to counteract the harming effect of induced drag.

Furthermore, once the final winglet had been chosen, the possibility of existing cavitation was analyzed and, after verifying that the working pressure was indeed higher than the vapor pressure, it was concluded that no cavitation phenomena had to be taken into account. Nevertheless, a brief research on the diverse methods that exist to protect watercrafts and machines from erosion caused by cavitation was made. Therefore, this project aimed to enumerate the most common ways to avoid cavitation, erosion and corrosion, and introduce some new methods that might ease the process and reduce costs; such as using Spry Elastomers that could be applied in-situ, and whose price was substantially less expensive than the ordinary methods.

In addition, bearing in mind the academic nature of this project and the limited amount of available time, this project also carried out a brief study of the possible materials that could be used in order to build a hypothetical model of a windsurfing board and its correspondent hydrofoil. After analyzing the working condition of the windsurfing board of the current project, among the most commonly used materials – which are fiberglass, EPS and Epoxy – it was concluded that Epoxy was the most

practical and economic option of all. Still, this project also introduced a brand new alternative: BioFoam, which is a revolutionary foam whose ingredients are purely based on plants, thus reaching considerably low values of carbon footprint.

To sum up, at the end of this project it can be concluded that the addition of a blended winglet with bias tip did indeed reduce the induced drag and increase lift, that no cavitation phenomena had to be taken into account, and that a model could easily be built with environmentally friendly materials.

Sumary.

Figures.

1. Preface.

This project aims to study the effects that derive from the addition of wingtip devices to a E211 hydrofoil, in order to reduce induced drag. On a secondary line, it briefly explores some cavitation resistent materials.

1.1. Origin of the project

Since the origin of life, human beings have spent innumerable hours in uncovering nature's mysteries and understanding the motivation than lies behind every phenomenon that surrounds them. It is highly probable that the first thoughts ever conceded to aerodynamics were born inside some inquisitive draft of an engineer that wondered about the functioning of a bird's flight, or the ease with which fishes swim through water. As time went by, this inclination towards the unknown has become the engine that promotes the evolution of life and awakens people's intellectual activity, leading them to the discovery of Aerodynamics.

Still, for some, Aerodynamics is not only a branch of Fluid Dynamics that studies the actions that result from the interaction between a solid body and the surrounding fluid, but, in a way, it represents the maximum expression of freedom. If not, why would some plain bicycle manufacturers from the EE.UU like Wilbur and Orville Wright decide to dedicate their lives to the aviation world, were it not for a biting necessity of freedom? But men do not only live from breathing. Water, in its many forms, has occupied many brilliant minds over the centuries, going from *20.000 Leagues under the Sea* by Jules Verne, to *The Old man and the Sea* by the Nobel Prize winner, Ernest Hemingway.

Therefore, thanks to aerodynamics, humanity can now understand Nature, and translate this knowledge into creations that may not only preserve Nature, but also benefits people's lives.

1.2. Motivation.

The main stimulus that lies behind this project is no other than the same that attacked many brilliant minds from the past: an urgent and acute hunger for knowledge.

Aerodynamics – in particular, hydrodynamics – has always appeared particularly attractive to my understanding. Being able to undestand, describe, analyze and design devices that could make the most of the fluid surrounding into which they are set has always been specially seductive; and when the opportunity to study the behavior that resulted from the additon of wingtip devices to an E211 hydrofoil came, I jumped into the project as soon as I could hoping to uncover many secrets and reach an acceptable understanding of Fluid Dynamics.

2. Introduction.

This project is based on *Hidrodinàmica i Aplicació dels hydrofoils al windsurf*, by Laura Voltà and Júlia Solanes. Therefore, it focuses on the optimization of the E211 hydrofoil by the addition of wingtip devices and a brief study of cavitation and some cavitation resistent materials.

2.1. Objectives.

The main objective of this project is to analyze the effects that derive from the addition of wingtip devices to a E211 hydrofoil, in order to optimize its performance by reducing the induced drag caused by wing tip vortices.

On a secondary line, it also presents a very brief study of some cavitation resistent materials and offers a couple of options in order to select the material that could be employed to build the E211 hydrofoil.

2.2. Scope.

This project only addresses the optimization of the E211 hydrofoil by the addition of wingtip devices, such as winglets. It does not include a study of the diverse wingtip devices, but simply focuses of a couple of them. In additon, it only explanis the cavitation phenomenon and presents some cavitation resistent materials; it does not study or analyze them. Finally, it presents a couple of materials that could be used to build the E211 hydrofoil, but does not build any model at any stage of the project.

3. Hydrofoils for windsurfing.

The main purpose of this chapter is to introduce the reader to the wide and still unknown world of hydrofoils. Firstly, in order to accomplish this task, a brief review of the history of the hydrofoils will be presented. Immediately following this section, the basic concepts where the workings of the hydrofoils are based upon will be explained. Also, on a parallel line, a short glimpse of the history and functioning of windsurfing will be given. Finally, the crucial phenomenon of the induced drag, its causes, consequences and solutions will be expounded.

3.1. Introduction of hydrofoils.

What the reader will encounter in this section is: firstly, a skin-deep inspection of the history of hydrofoils; secondly, an exposition of the functioning of the hydrofoils; and lastly, a general presentation of the diverse employments of hydrofoils.

The background of hydrofoils.

The first known instance of a hydrofoil grounded vessel was a catamaran, which included four transverse *hydroplanes*, designed by Comte de Lambert in 1897. In 1898, an Italian man called Forlanini developed a ladder type hydrofoil craft which surely flew of the water. However, little record of the doings of these ships was preserved.

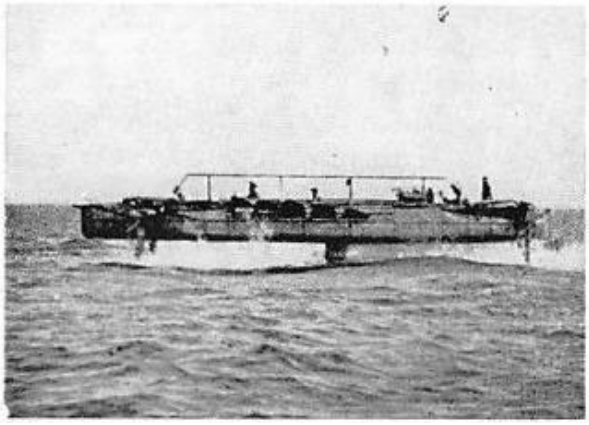

Figure 1. Forlanini's ladder type Hydrofoil[(1)].

Subsequently, by 1907, the first Americans of certain renown to experiment with hydrofoil supported craft were Wilbur and Orville Wright – commonly

known as the Wright Brothers, the inventors of the plane as it is known nowadays – who also based their analysis in the behavior of a catamaran. However, due to some unrecorded impediments, their efforts were ill rewarded and the experiment had to be put to an end quite early [Bob Harris][(1)]. In 1918, the endeavors of Dr. Graham Bell – the inventor of the phone – and his collaborator Casey Baldwin resulted into the inception of the HD-4. Baldwin's passion for boating might have been what triggered the late sudden interest of Bell towards hydrofoils. Somewhere in the middle of October 1906, Bell asked himself : *why shouldn't we have heavier than water machines as well as lighter than water machines?* After a couple of setbacks, Bell and Balwin managed to design and build the HD-4, which was nothing less than what they called a *hydrodrome* that incorporated all that had been learned from previous successes and failures. It performed well; rising easily, accelerating rapidly, taking waves with little or no difficulty, demonstrating good stability, etc.

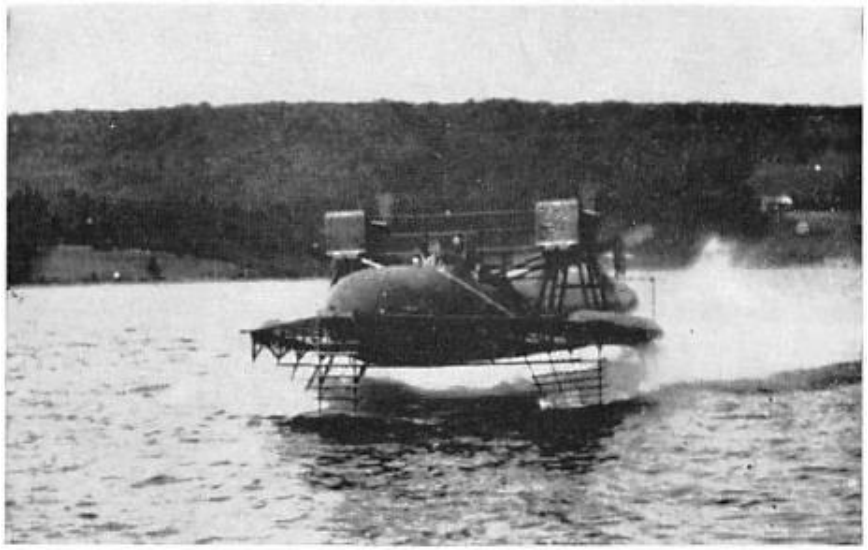

Figure 2. Bell and Baldwin's HD-4 Hydrodome[(2)].

A year later, Bell had the fortune to gain the attention from both the British Admiralty and the United States Navy. Both delegations reported enthusiastic statements; but in the end, neither considered it opportune to place an order. Eventually, the HD-4 was dismantled a year before Bell's death. [Robert V. Bruce, 1990][(2)].

Years passed and hydrofoils were slowly starting to become rather popular among the US and the Canadian Navy. A Canadian Navy's experimental hydrofoil, for instance, could reach 96 km/h by 1954. In 1957, Christopher Hook's Hydrofin arrived. It represented a near answer to the problem of hydrofoil craft in most circumstances of wind and sea, but there still remained an urgent need and desire for simplicity, low maintenance, light weight and better retraction quality. Gordon Baker – who was living and working in the US during this very same time – had been developing hydrofoil craft with surface piercing foils of a dihedral greater than 30º. One of his first models was a hydrofoil sailing craft. The system was constituted by two surface piercing V foils and a single V foil aft.

Figure 3. James Gorgono's Icarus[4].

However, despite performing well once up on the foils, the sailboat could come down off the foils as soon as the wind faded. After a couple of troubles that forced him into an involuntary delay, Baker designed the Highpockets, which consisted of four sets of surface piercing V foils with 50% of the load distributed on each pair. Finally, he invented the Monitor, which belonged to the ladder foil category [Owen Dumpleton, 1956][3]. Thanks to many innovations, the Monitor managed to achieve a speed of 38 knots.

Around 1969, James Grogono invented the first hydrofoil conversion of a standard sailing catamaran: the Icarus. The distinct feature of Gorgono's contribution was the so long-desired simplicity. Sailing on hydrofoils, if successful, could certainly lead to very high speed. [James Grogono, December 1987][(4)]

Figure 4. A recent example of Russian boats with hydrofoils[(5)].

The fluid dynamics involved in hydrofoil design is complex, but in his article published in August 1970, Grogono detailed a guide line which would help avoid many practical errors. The Icarus embraced all these factors, which is probably the main reason why the craft managed to achieve a speed of 21.5 knots during the celebration of the first Speed Week, held at Weymouth, UK. With her new metal foils, the Icarus was the fastest hydrofoil of the competition and she reached the mentioned 21.5 knots over the 500m course.

From then onwards, hydrofoils emerged as a rising interest in the Sovient Union. This engagement, however, had already begun with the Raketa (Rocket), a 60-person passenger hydrofoil, which was in serial production between 1957 and 1976. It cruised at 60 km/h with a 500 km range. The larger, Meteor-type Soviet hydrofoil was in production from 1960-1994; its speed was 66 km/h and it could carry 112-123 passengers. The military field became interested in the hydrofoils too; leading to the design of the Soviet Turya-class fast attack torpedo b oats, which were in service starting in 1972. On

a parallel line, Boeing design and built several hydrofoil craft for the U.S. Navy from the early 1970s to the current times.

Figure 5. Streamlines around a hydrofoil.

Nowadays, modern designs are being built, not only for military or experimental purposes, but also for pure enjoyment of those who relish for a fast cruise. The FSWH37, for example, is an Italian made hydrofoil; completely build in aluminum alloy, except for the foils which are in high resistance steel. The latest hydrofoil boats come from Russia. Glass bottom boats as the Looker seem to revive the hydrofoil technology so there is solid hope for a bright future for the hydrofoils.

3.2. Functioning of a hydrofoil.

A hydrofoil is a thin sheet of material completely or partially submerged in flowing water. It has all the main characteristics of an airfoil working in the air, but due to the thicker nature of water, the forces produced by a hydrofoil are considerably greater that those produced by an airfoil of the same size and shape.

The main value of a hydrofoil is essentially its ability to generate an acting force almost at right angle to the direction of the water flowing across it, and this force is substantially bigger than drag, or the resistance of the foil to the water flow. Thereby, if a force to act on a boat which is travelling through the water is needed, a hydrofoil can always be attached to the boat in order to obtain it.

As observed in Figure 5, the lines – called *Streamlines* – are the directions in which particles of water travel. It is clearly appreciated that the water flowing past is turned from its course. Now, when this occurs, a force is acting upon the water, and in this case, it means that the foil is exerting a force on it.

Since action and reaction are equal and opposite, the water is also exerting a force on the hydrofoil.

If one regards with attention Figure 5 once again, it is noticeable that above the foils, the streamlines are crowded closer together indicating that the water is flowing faster there. In contraposition, below the hydrofoil, they are widely separated indicating that the water flow is considerably slower. According to Beroulli's theorem, those sections of flow where speed is higher, signify low values of pressure; and those sections with separated streamlines; that is, slow speeds, imply higher pressures. This gradient of pressures is what causes airfoils to fly and hydrofoils to elevate of water.

Incidentally, it must be kept in mind that hydrofoils are lifting profiles employed in water whose shape, structure and functioning share a deep resemblance to those of an airfoil. The term *lifting* may be regarded as a description of the vertical force produced by these profiles when advancing in a fluid; and this very same concept comes to the public from aerodynamics, where *lift* is the force exerted on an air craft by wings to raise it off the ground [Robert B. Harris, June 1958][(5)].

3.3. The design of hydrofoils.

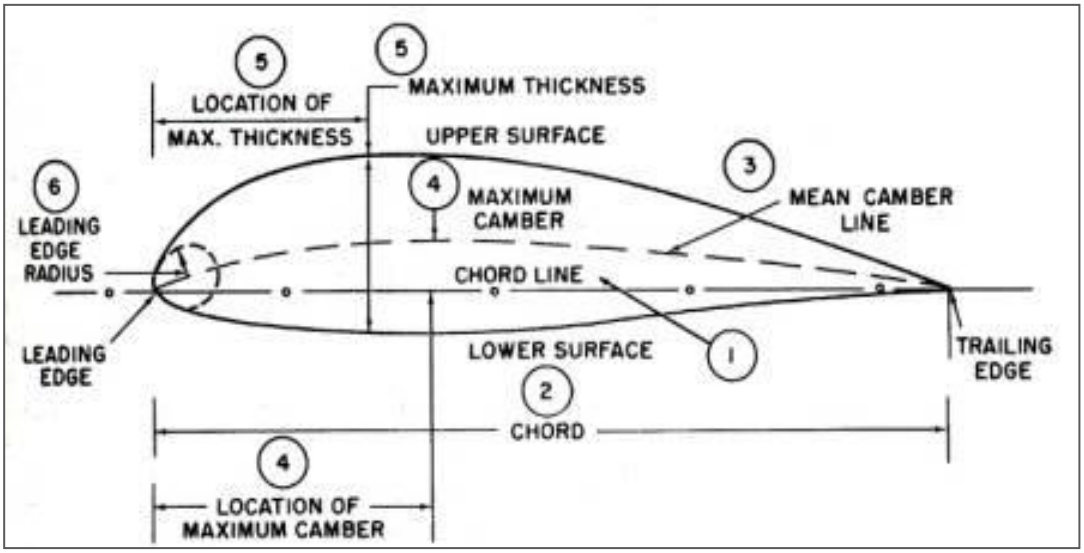

Figure 6. Main constituting parts of a hydrofoil[6].

Hydrofoils are one of the most exciting prospects for the further advancement of sailing. There are two configurations of hydrofoils: the surface-piercing hydrofoils and the fully submerged. Bearing in mind the nature of windsurfing boards, this project focuses of the last type.

This said, it is imperative to say that however different these two configurations may be, the share many commonalities; such as the chief points in the design of profiles [John Morwood, 1958][6].

Hydrofoil profile: it is the section of a wing; that is to say, what one would see were the wing sliced transversely. Except in the particular case of rectangular wings, in which all the profiles of the wing share exactly the same shape, it is usual that profiles present diverse geometries; trimming down as one reaches the tip of the wing.

Leading edge: it is the front edge of the wing; that is, the line that joins the front section of all the profiles that comprise the wing; or in other words, the first area of the wing that impacts against the flow.

Trailing edge: it is the rear edge of the wing; that is, the line that joins the posterior section of all the profiles that comprise the wing; or in other words, the area of the wing where the deflected flow returns to the free stream.

Extrados: it is the superior section of the wing contained between the leading edge and the trailing edge.

Intrados: it is the inferior section of the wing contained between the leading edge and the trailing edge.

Thickness: maximum distance between extrados and intrados. The thicker foils will dispense more lift and therefore, might get the craft off the water more quickly. But they will also produce hire values of drag as well, and they may cavitate sooner. In *The Design of Hydrofoils* written by John Morwood in 1958[(6)], he recommends that a ratio of 10:1 might prove better for sailing crafts which are not to reach important speeds.

Chord line: it is the imaginary straight line drawn between the leading edge and the trailing edge of every profile.

Mean or camber line: wing profiles are not always symmetric but they trim down towards the tip of the wing. The same thing happens to the chord, which characteristic of every profile. In order not to talk about a different chord every time, a mean chord is used.

The line of the 25% of the chord: it is the imaginary line that would result from joining every single point located at a distance of a 25% of the length of the chord of all the profiles that comprise the wing.

Camber: the superior curvature refers to extrados; the inferior curvature refers to intrados. The mean curvature is equidistant from both surfaces. It is usually expressed in percentage.

Wing Surface: total surface of the wings.

Angle of Attack (α): as a foil moves through a fluid, it is inclined to the movement direction at a certain angle. This is the angle between the chord line and the movement direction, which is called

angle of attack and has a large effect on the lift generated by the foil. For thin airfoils ad hydrofoils, lift is directly proportional to the angle of attack for small angle (within aprox. 10º). For higher angles, lift suffers an abrupt decrease due to the separation of the boundary layer. This condition is called win stall.

3.4. Lift and Drag Forces and Coefficients:

Aerodynamic forces result from the pressure distribution over a surface. On a hydrofoil – as well as an aircraft in flight – four main forces act on it: Thrust, Drag, Lift and Weight. This section will address only Lift and Drag.

3.5. Lift.

Lift is the force that directly opposes the weight of a craft and elevates the ship of the water. The direction of this force is always perpendicular to the direction of the speed of the incident water flow. The mathematical expression that models lift is expressed as follows:

$$F_L = \frac{1}{2}\rho u^2 c \cdot C_L \quad \textbf{(eq. 1)}$$

F_L is the Lift Force [N].

ρ is the density of the fluid [kg/m^3].

u is the speed of the fluid [m/s].

c is the length of the chord of the profile [m].

C_L is the lift coefficient in 2D [no dimension].

There are two mechanisms employed to generate Lift. The first one is the use of an **asymmetric profile.** It is often used for subsonic applications. The second one is the adoption of a certain angle of inclination relative to horizontal, which is the angle of attack. For low values of this angle, the flow remains attached on both surfaces. For higher angles of attack, reparation occurs, which leads to substantial increases of drag and decreases of lift. Eventually, the hydrofoil will reach a stall condition where the pressure distribution on the top and bottom are equal [Dr. J. M. Meyers, Dr. D.G. Fletcher, Dr. Y. Dubief][7]. Lift is the main responsible to avoid the craft to sink or drifts its navigation course.

3.6. Lift Coefficient.

As the rest of the aerodynamic coefficients, the lift coefficient has no dimension. The mathematical formula that describes its functioning is expressed as follows:

$$C_L = \frac{2F_L}{\rho u^2 c} \quad \textbf{(eq.2)}$$

The value of this parameter indicates the magnitude of the Lift Force of the profile. It is characteristic of every analysed profile; therefore, it is extremely useful to study its evolution based on the diverse angles of attack..

3.7. Drag.

Drag is the aerodynamic force that opposes a craft's motion through water. In consequence, the direction of drag is always opposed to that of the speed of the fluid. This is precisely why it is also often referred as fluid resistance, as it impedes the advancement of the body through the studied fluid.

This sort of resistance is comprised of two components: the profile drag and the induced drag. The latter will be expanded in section 5. Regarding the former, the profile drag is the resistance directly caused by the friction between the fluid and the foil surface, which is due to the fluid's viscosity. The following expression illustrated the functioning of this sort of drag.

$$F_d = \frac{1}{2}\rho u^2 C_D c \quad \textbf{(eq. 3)}$$

Where:

F_D is the Drag Force [N].

ρ is the density of the fluid [kg/m^3].

u is the speed of the fluid [m/s].

c is the length of the chord of the profile [m].

C_D is the drag coefficient in 2D [no dimension].

3.7.1. Drag coefficient.

The drag coefficient is deduced from eq. 3, and it stands as follows:

$$C_D = \frac{2F_D}{\rho u^2 c} \quad \textbf{(eq. 4)}$$

4. Hydrofoil Windsurfing.

The aim of this section is to introduce the reader into the world of Windsurfing by briefly exposing its background, and explaining its current relationship with hydrofoils.

4.1. A brief history of Windsurfing.

Windsurfing has become one of the most popular sports around the world; however, it all started with an idea. In 1948, when Newman Darby – a 20 year old American – invented a floating platform, which reminded more of a catamaran than the current idea of what we consider a windsurfing board, on which he mounted a sail. He called his creation *sailboarding*, after he wrote an article in 1965; however, he never patented it.

In the mid-sixties, Jim Drake – who was an aircraft engineer – ponder the idea of some sort of water ski that could float when somebody stood on it, and which would be driven not by a boat, but by a wind filled kite which could be steered by hand. Being good friends with his neighbor Hoyle Schweitzer, he discussed his idea with him and both started working on it. They called their invention many different names after finally reaching one that they truly enjoyed: the windsurfer. In 1970, they patented the windsurfer, but Jim Drake did not seem convinced with it and decided to sell the patent to Hoyle, who changed the name into *windsurfing international* and eventually earned millions with his invention. Hoyle was producing polyethylene sailboards in big quantities and the *windsurfer international* soon turned out to be a huge success, especially in Europe. During those ages, windsurfing became a booming business and in consequence, many different new brands were founded. Some of them, such as Mistral or F2, are still on the windsurfing market nowadays.

The late seventies and the early eighties were the booming ages of windsurfing. With its popularity, the development did not stand still either, and a lot of new ideas were introduced, even more brands

were founded and the professional windsurfing association was born.

Therefore, windsurfing slowly underwent a steady growth from a trend to into an official sport. Eventually, by 1984 windsurfing was accepted as an Olympic sport. This very same year, the Olympics were held in Los Angeles, USA, where Stephen van der Berg won the first Gold Medal. In 1992, during the celebration of the Olympics in Barcelona, Spain, women were allowed to compete in the windsurfing class. Barbara Kendall won the first ever female windsurfing Olympic Gold Medal.

Figure 7. AHD ASF-1 windsurfing board [20].

Over the years, the history of windsurfing has witness the birth and death of many different disciplines. Some of them are the *Slalom windsurfing*, the *Freestyle*, and the most spectacular discipline of all: the *waveriding* or *wave performance*.

4.2. Hydrofoils applications.

As many other watercrafts in history, the windsurfing board has also had the chance to experiment with hydrofoils. Speed is a necessity in an Olympic sport where professionals compete in order to earn the so-desired Gold Medal. Therefore, any device that might aid the windsurfers increase their velocity is desperately hunted by those who design the boards.

True to this commitment, many brands have been experimenting on new methods to attach especially designed hydrofoils to windsurfing boards. However, it is the AHD – a French brand specialized on windsurfing – who entered, years ago, a series of tests and trials and eventually launched their own foiling machine: the AFS-1, in 2012.

As stated by the AHD Team, the AHD ASF-1 is clearly the only hydrofoil to have been particularly designed and developed for the constraints and specificities in windsurfing.

This board is particular in the sense that its shape is quite surprising. The foil's fuselage is voluminous, which helps the windsurfer to take-off earlier. Wings are also wide, their profiles are thick, their twist carefully designed to enhance power, lift and stability. The winglets regulate the water flow on the wings in order to maximize power and generate the lift needed for taking off easily and earlier. Finally, it is 100% made of carbon fiber, and it has a flat bottom and an enhanced volume at the tail.

5. Induced Drag.

The main purpose of this section is to define the phenomenon of Induced Drag by presenting its causes and consequences, and introducing diverse solutions that have been proposed over the years in order to reduce it.

5.1. Definition.

Aerodynamic drag generally consists of friction drag and pressure drag. Friction drag is determined almost entirely by the state of the boundary layer – laminar, transition or turbulent – and does not vary much between subsonic and supersonic flow. Whether as Pressure drag increases substantially at supersonic speed due to shock waves, which is the reason why is it sometimes called "wave drag".

Aerodynamic drag is also divided into zero-lift drag and lift-dependent drag components. In general, drag is treated approximately as zero-lift drag since friction drag is not sensitive in the change of angle of attack. Within the lift-dependent drag section, there are two types of drag: the wave drag due to lift, which manifests itself in supersonic flows; and a component called **induced drag**, which appears at subsonic speed [Mohsen Jahanmir, 2011][8].

Figure 8. An example of the wingtip vortices on a flying airplane[8].

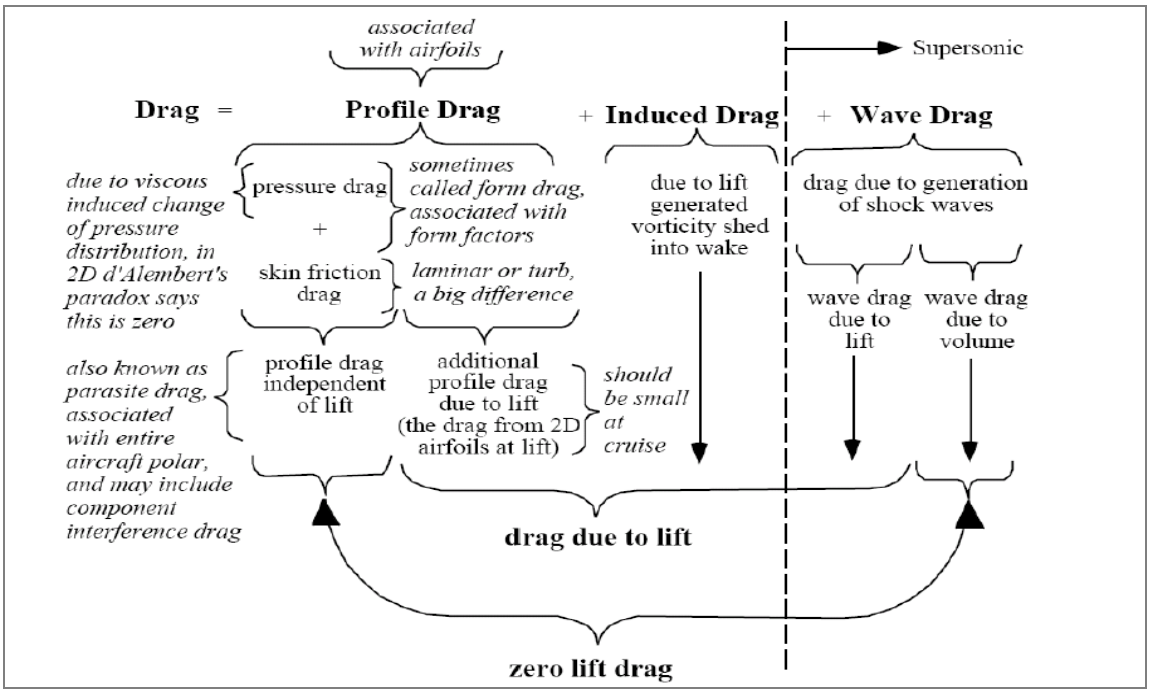

Figure 9. Main constitutors of Total Drag[11].

Induced drag arises primarily because the lift produces circulation around the wing, which leads to a sheet of twirling vorticity in the wake and results into counterrotating vortices (Figure 11).

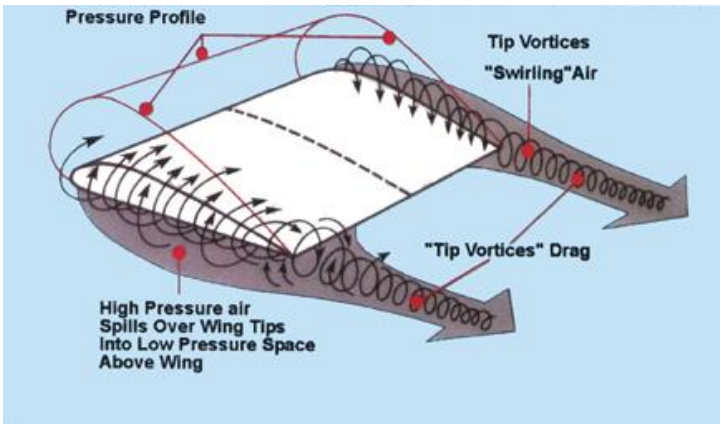

Figure 10. Example of wingtip vortices[11].

The difference in water pressure between the lower and the upper surfaces of a wing causes the water to escape around the wingtip, which reduces the available lift.

The motion of the water rushing around the wingtip, together with the velocity of the flow through which the hydrofoil is travelling, causes a vortex to form near the wingtip, as shown in Figure 11. The tip vortices cause upwash and downwash water currents that alter the direction of the free stream flow around the hydrofoil.

5.2. Background.

Since the early seventies and the subsequent trend in world fuel prices, drag reduction technology has become of prime priority. Still, the importance of and possibilities for viscous drag reductions were first identified in the late 1930s. The economic viability and future survival of an aircraft or a watercraft depends on minimizing aerodynamic drag, while maintaining good handling conditions. In addition, drag reduction has a wide range of positive ramifications, such as: reduced fuel consumption, larger operational range, greater endurance and higher achievable speeds. Still, as it has been previously stated, drag is constituted of diverse components, which implies that, if a significant reduction of drag is desired, it will be necessary to properly analyze and address each one of them.

For instance, when analyzing the skin friction drag reduction, two methods are generally considered: the first one aims at reducing the turbulent skin friction, while the second one aims at delaying transition to maintain large extent of laminar flow, as did the earliest research in aeronautical viscous drag reduction back in the early 1930s (Figure12 and Figure 13).

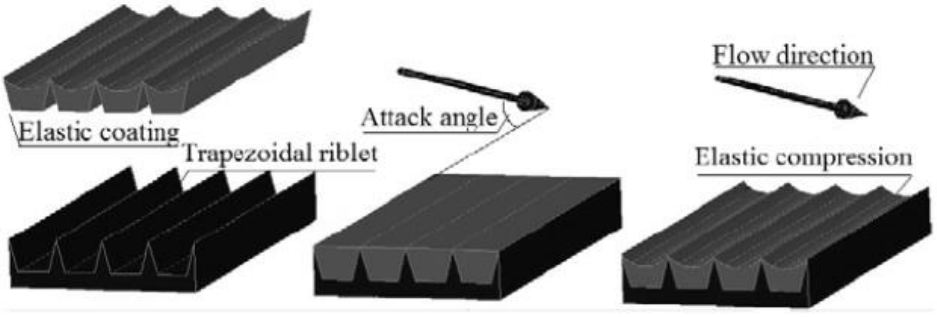

Figure 11. Example of diverse methods to reduce skin friction[12].

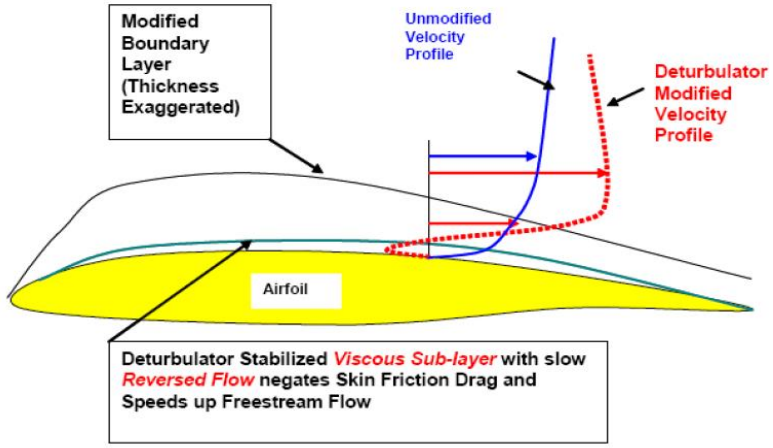

Figure 12. Trying to delay the separation of the boundary layer[(12)].

5.3. Wing span, Aspect Ratio: Induced Drag Equation.

However, as it has been already stated, there is another major component: lift-induced drag. The upwash effect of the tip vortices that cause induced drag has its greatest influence on the wing section closest to the tip. If the wingtips are pushed outboard – therefore increasing the wing span – a smaller section of the wing will be affected by the tip vortices. What inevitably follows this reasoning is that if a span were infinite, induced drag would be zero because there would be no wingtip; therefore, no tip vortex to create induce drag. This endless increasing of the wingspan leads to the classical way to decrease the lift-induced drag: the **aspect ratio** of the wing [Mohsen Jahamir, 2011][(8)].

As it is known, the aspect ratio (AR) is a measure of how long and slender a wing is from tip to tip, and it is defined to be the square of the span divided by the wing area (b^2/s). Therefore, high AR values imply long and slender wings, whether as low AR values imply short and wide wings. Considering the mathematical expression that describes the AR, it is obvious that the higher the AR is, the lower the induced drag becomes. On the other hand, low AR values indicate wider and shorter wings, which imply higher values of induced drag. The following equation illustrates the influence that the AR and the wingspan have in the calculation of Induced Drag.

$$C_{Di} = \frac{C_L^2}{\pi \cdot AR \cdot e_0} \qquad \textbf{(eq. 6)}$$

C_{Di} Induced Drag.

C_L Lift coefficient.

AR Aspect ratio.

e_0 Oswald efficiency number.

As equation 6 suggests, induced drag depends on the aspect ratio and the lift coefficient. Therefore, the bigger the AR is, or the smaller the C_L gets, the smaller will induced drag get.

Still, while it is true that high AR values produce less lift-induced drag, it is essential to mark that they also cause higher parasitic drag –which is a combination of form drag, skin friction drag and interference drag. However, the increase of parasitic drag is small compared to the variations that the induced drag suffers; but given that the aspect ratio is also a compromise between aerodynamic and structure characteristics, it is clear that for a given technology, there is not a great possibility to increase it without affecting the wing structure. Given that this project is based upon *Hidrodinàmica i aplicació dels hydrofoils al windsurf* by Laura Voltà and Júlia Solanes [(9)], at a certain point, it was considered to preserve the AR = 3,75 that they chose. Still, given that the aim of this project was to reduce induced drag, which was precisely achieved by the addition of winglets as well as increasing the aspect ratio, the final AR chosen was 7,1. An AR of 7,1 was deemed to be appropriate because the desire for high aspect ratio and optimum aerodynamic efficiency had to be balanced against material-stregth-to-wieght ratior, overll weight of the hydrofoil, etc. For all these reasons, the best aspect ratio for the average hydrofoil might be seven or eight to one[(23)].

Therefore, since induced drag is manifested in the wake as a rotational kinetic energy, the alternative is to develop wing tip devices acting on the tip vortex that would help overcome this phenomenon.

5.4. Wingtip devices: the solution.

Stretching wingspan or increasing aspect ratio certainly reduces induced drag. Designers, though, have to balance the benefits of less induced drag against the costs of structural weight increases, more parasitic drag or cost considerations. Therefore, apart from the classical ways to reduce lift-induced drag; that is, increase aspect ratio or wing span, there are other methods.

According to Bushnell [Bushnell, 2003][(10)], there are two approaches for reduction of induced drag.

1) **Energy extraction from the tip vortex:** devices can be inserted into the flow, like tip turbines for energy extraction, winglets, tip sails, among many other.
2) **Alternation of tip boundary condition(s):** these lift dependent drag reduction techniques are based upon either eliminating the tip entirely, or adding mass in the tip region.

In particular, this project centers its attention to the adding of winglets which, along with reducing induced drag, imply many other advantages.

The idea of a beneficial wingtip appendage, or "wingtip device", has been around since the early 20th century, when theoretical calculations first indicated that a vertical endplate added to a wingtip would reduce the induced drag. Still, Whitcomb (21 February 1929 – 19 October 2009) seems to have been the first to recognize that it is possible to obtain real tangible results of adding a wingtip device.

From an aerodynamic point of view, the motivation behind all wingtip devices is to reduce induced drag. Under these lines follows a list of the potential benefits of tip devices, in rough order of importance, and some offsetting factors:

Benefits:

- Improved performance:
    - Reduced fuel burn – in case of aircrafts or water crafts, such as boats.
    - Increased maximum range.
    - Reduced takeoff field length.
    - Increased cruise altitude.
    - Increased cruise speed.
- Meet gate clearance with minimal performance penalty.
- Appearance and product differentiation.

Offsetting factors:

- Increased cost (development, recurring and purchase).
- Increased development risk.

Another possible benefit that has sometimes been put forward is that tip devices can reduce the strength of the vortex wake, which could lead to improved safety. The main positive factor that makes the benefits possible is the reduction of induced drag.

5.5. Types of winglets.

Whitcomb's breaking of the "endplate paradigm" has led to the development of a variety of wingtip devices that can be effective in reducing total drag, some of which are detailed under these lines. Basic strategies for practical devices:

- Increasing horizontal span.
- Going nonplanar:
    - Bending (winglets).
    - Bending with blending (blended winglets reduced with less wetted area pentalty).

- Splitting (split winglets and feathers).
- Splitting and rejoining (spiroids).

- Part-chord devices (less chord than the baseline winglet).
- Pronounced tapering.
- Additional sweep.

This project focuses on the Non-planar wingtip devices because, as I. Kroo from Stanford University states in *Nonplanar wing concepts for increased aircraft efficiency* [(11)], they offer the possibility of reduced drag compared with planar wings of the same span and lift. While it is true that induced drag may easily be reduced by increasing the span of a planar wing, they imply higher weight and cost, and non-planar devices allow not only less cost, but also the possibility of improved stability and control characteristics.

In particular, it focuses on winglets, which are devices attached at the wingtips, used to improve efficiency by lowering the induced drag caused by wingtip vortices. They work by increasing the effective aspect ratio of the hydrofoil without adding great weight to the structure.

Figure 14 depicts some of the diverse types of winglets that exist. For instance, the Supermarine Spitfire (WWII) already used elliptical wings.

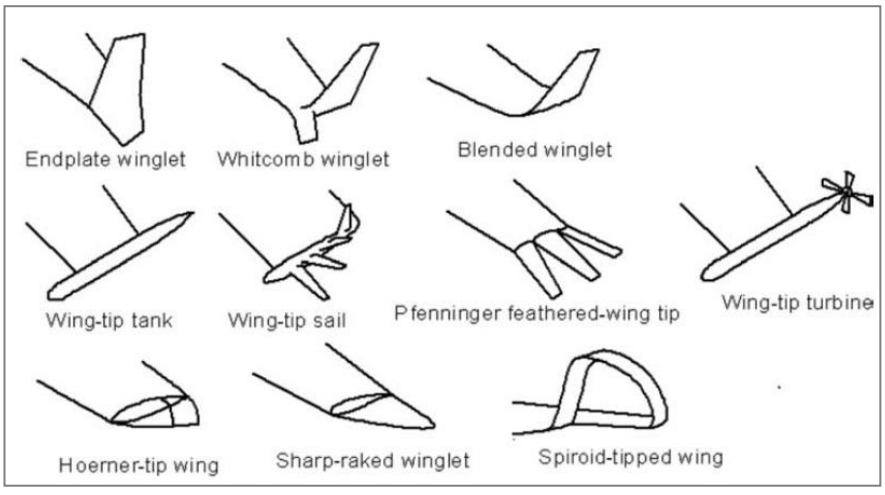

Figure 13. Examples of the many winglets that exist.

Now, the usual procedure in design studies is to define the general configuration of a candidate tip device in terms of its planform and dihedral angle(s), and then estimate its performance through analysis. In order to start the study to find the proper wingtip device that had to be attached to the hydrofoil E211 so that an optimization by a sensible reduction of induced drag was possible, it was necessary to discern which was(were) the best option(s) by analyzing the diverse results that the many wingtip devices offer.

5.6. Selection of the right winglet.

Basing on a study carried out by Doug McLean[(12)], a comparison between the stated wingtip devices demonstrated that, as the thumb rule suggested by Whitcomb affirms, for a given device, a horizontal extension is nearly twice as powerful as a vertical one, both in terms of drag reduction and weight increase. So in terms of the trade between drag reduction and weight increase, horizontal span extensions and vertical winglets have practically the same performance potential.

Given that the device's size criteria did not offer any hint about which kind of wingtip device is better, Doug also considered taking induced drag, profile drag and wing structural weight into account, but neither of these parameters seemed to definitively highlight one wingtip device over the others. Thus looking at just the reduction in drag, the improvement in L/D or aspect ratio is not sufficient when evaluating the benefits of wingtip devices.

Therefore, considering the results of the numerous studies carried out by Doug, a variety of tip-device configurations have been identified as potentially beneficial, and analyses that take all the relevant factors into account have not found any configuration to have any pronounced general advantage over the others; since inherent differences in the optimized results are small.

In order to properly analyze the diverse options that might influence over the reduction of induced drag, it was considered to model several existing winglet designs and simulate their behavior, so that the best of them could be selected and studied. Some of these designs were not only winglets, but also endplates or elliptical wings. Therefore, the main studied designs were:

- Endplates.
- Blended winglet with bias tip.
- Blended winglet with not bias tip.
- Elliptical wing.

Figure 14. Blended winglet, elliptical wing, endplate winglet, blended winglet (no bias tip) [12][14].

Figure 15 depicts four examples of the analyzed winglets. However, there still was a hindrance to overcome: the design of the winglets itself. In order to choose the right dimensions, it was necessary to follow some criteria that dictated which dimensions had to be used when modelling every winglet. Whitcomb's design was the one that offered more data and it was the pattern that was eventually followed.

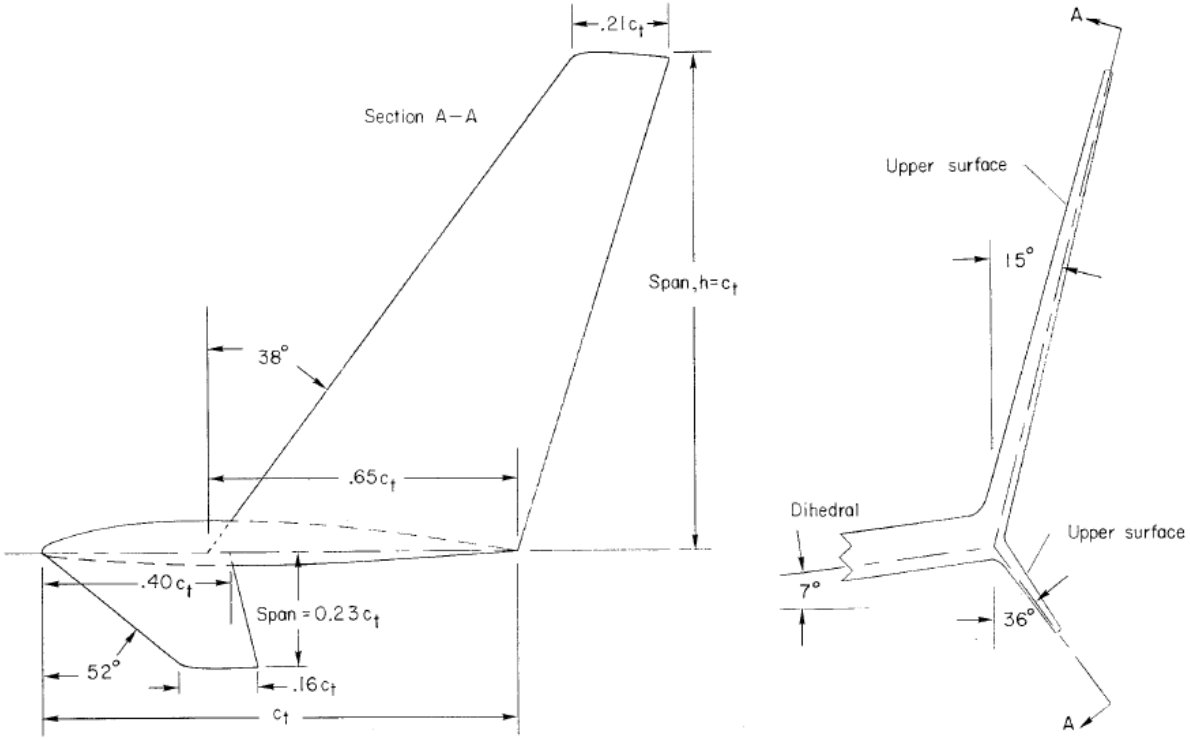

Figure 15. Whitcomb's winglet design measurements[12].

Still, the complexity of the design was considerable, and only some measurements were considered; such as the angles of inclination of the winglet, or the span. Figure 16 depicts a real example of Whitcomb's design.

Figure 16. Whitcomb's design applied to a flying airplane[14].

6. Numerical Simulation: introduction.

The central task in the natural sciences lies in describing reality as accurately as possible in order to better understand natural phenomena, and thus gain insight into the behavior of objects under given conditions. In the past, there have been two methodical approaches: the practical and the theoretical. The first one converts the laws of nature to relationships between mathematical quantities, while the latter one implies performing physical experiments. Still, they both have their shortcomings. Therefore, besides the practical and theoretical approaches, **numerical simulation** has established itself in recent years as a third approach connecting the two traditional ones.

Numerical simulation is characterized by the discretization of mathematical equations that describe the behavior of the real world, and their subsequent approximate solution. By doing so, many shortcomings of both the experimental and the theoretical approaches are overcome, access to phenomena that otherwise could not be examined can be made possible, and experiments can be avoided.

6.1. Stages of a Numerical Simulation.

The following figure presents the different stages of a numerical simulation.

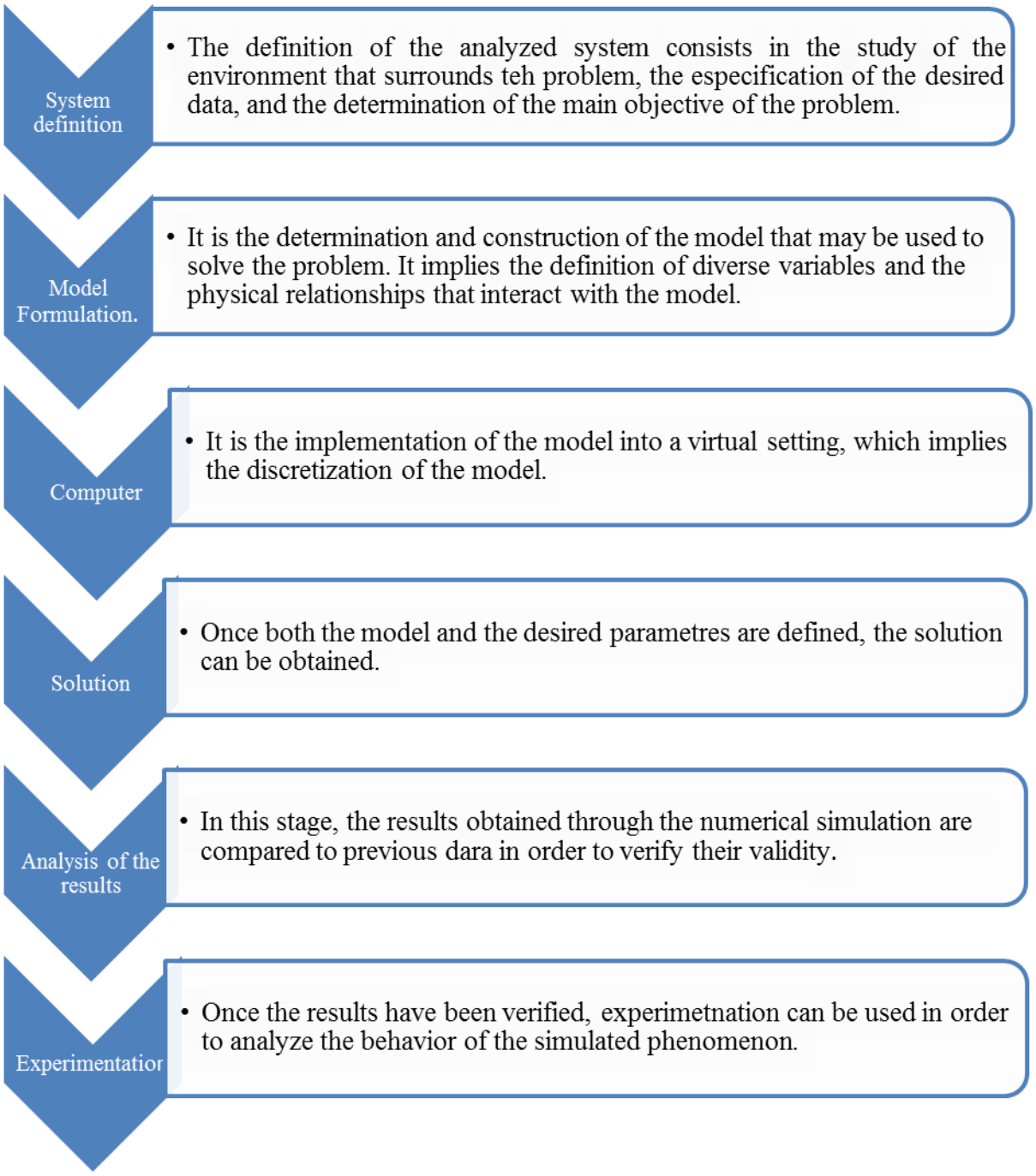

Figure 17. Diagram of the stages of a numerical simulation.

6.2. ANSYS Fluent.

While it is true that there are many numerical simulators for aerodynamic/hydrodynamic studies, ANSYS Fluent provides comprehensive modeling capabilities for a wide range of incompressible and compressible, laminar and turbulent fluid flow problems.. Robust and accurate turbulence models are a vital component of the ANSYS Fluent suite of models, and they have a wide range of applicability.

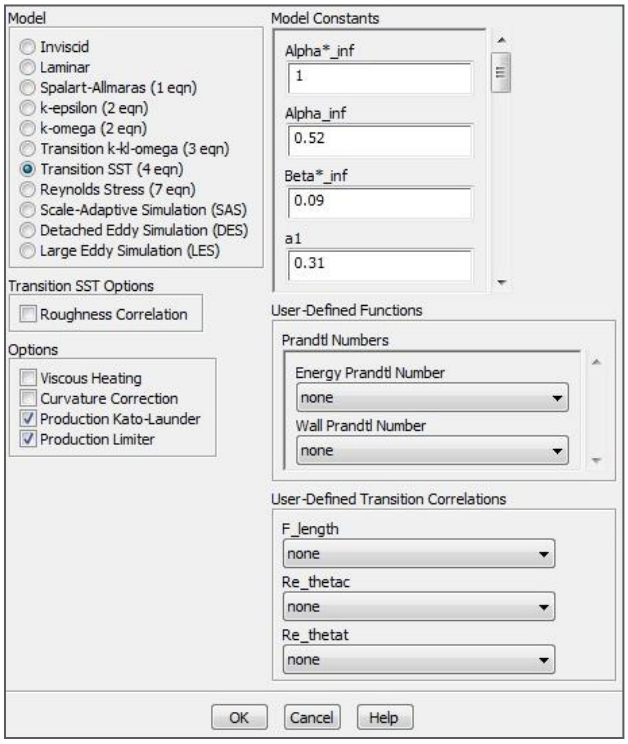

Figure 18. Selecting the SST model to start simulations.

One particular model is the **Shear-Stress Transport (SST)**, which was developed to effectively blend the robust and accurate formulation of the *k-ω model* with the freestream independence of the *k-ε model;* giving birth to a more complete model that embraces the best features of both *k-ω model* and *k-ε model*. Even though the SST model resembles the *k-ω model*, it differs in certain aspects – which are extensively addressed in the Annex A - which make the SST model more accurate and reliable for a wider class of flows, than the standard k-w model. Bearing these considerations in mid, the SST has been deemed to be the most suitable model to analyze the current project.

7. Numerical Simulation: analyses of the models.

In order to be able to properly analyze the effects that derive from adding a wingtip device to a hydrofoil, it has been considered that a 3D numerical simulation was the best option. Therefore, this section focuses on the generation of the diverse geometries with SolidWorks, their subsequent simulation in ANSYS Fluent, and the final selection of the profile that presents better results.

7.1. Geometry generation.

Given the fact that this project is based upon *Hidrodinàmica i apliació dels hidrofoils al windsurf*, by Laura Voltà i Júlia Solanes[9], the hydrofoil profile has already been established, so that the subsequent analyses were made upon modifications of the specified profile: the E211.

The following table presents the characteristic parameters and dimensions the E211.

Dimensions and characteristics of the E211 hydrofoil		
Chord (c)	0,1	m
Width	0,450	m
Area of lift (A_L) = b·c	0,0450	m
Thickness (t)	0,0113	m
Volume	0,000276	m^3
ρ_{Epoxy}	1150	kg/m^3
Velocity	12	m/s

Once having established the profile, it is important to remember that the main objective of this project was to modify the specified profile so that there is a reduction of the induced drag. As it has been previously stated, this reduction had to be accomplished by adding wingtip devices; so diverse designs were analyzed in order to compare their contribution to the final reduction of induced drag.

7.2. SolidWorks.

Based on the original E211 naked model, several modifications have been carried out in order to obtain the both the horizontal winglet, and the blended winglet. Importing the E211 profile from Airfoil Database[22], and using the solid modelling computer-aided design (CAD) and computer aided-engineering (CAE) software *SolidWorks*, several complex geometries can be generated. Figures 20 to 23 depict some of the final geometries.

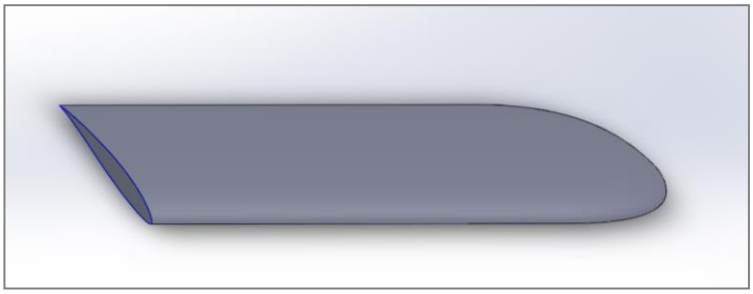

Figure 19. Elliptical.

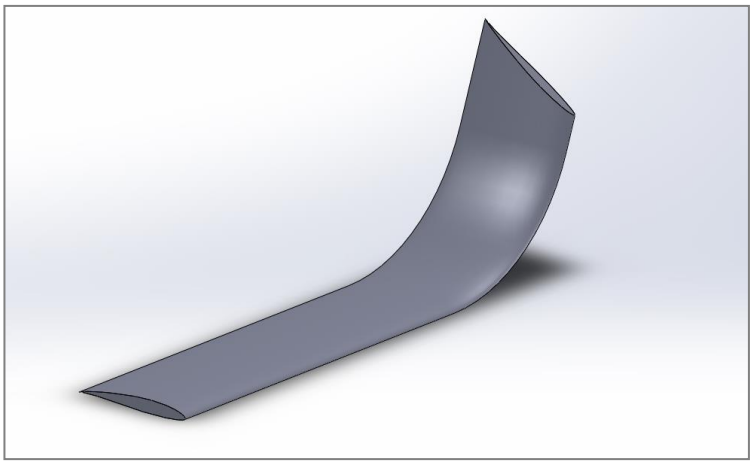

Figure 20. Blended with bias tip.

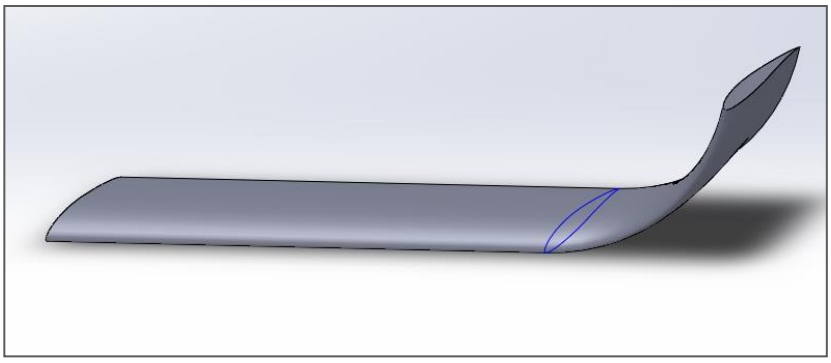

.

Figure 21. Blended with no bias tip.

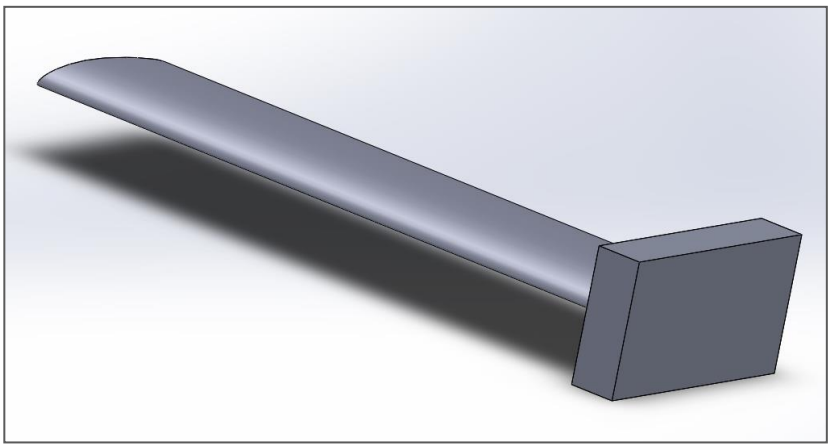

Figure 22. Endplate winglet.

Once the SolidWorks models were made, they were saved under an IGES format so that they could easily be imported to ANSYS Workbench Model Designer. Using the *Enclosure* and the *Boolean* tools, the geometry of both models was edited and eventually imported to the Mesh Editor.

Still, before the Mesh stage is addressed, it is interesting to understand what was done in the Model Designer and why it was done. First, the *Enclosure* tool creates surrounding regions around bodies to facilitate simulation of field regions. Therefore, it was used to simulate the surrounding fluid – water – that acted upon the hydrofoil. In addition, its name was changed to *Fluid* so that no later misunderstandings may arise from its nomenclature. Also, it was generated as non-uniform so that the dimensions were slightly bigger than those of the E211. This allowed the graphic results of the simulations to be clearer.

Second, the *Boolean* operator was employed in order to be able to select the two now existing bodies – enclosure and E211 – and subtract the latter to the first one, so that the meshing process could be started.

The following figures illustrate the stated process. Figure 24 depicts the geometry just after generating the Enclosure, while Figure 25 shows the blended winglet geometry after applying the Boolean operator.

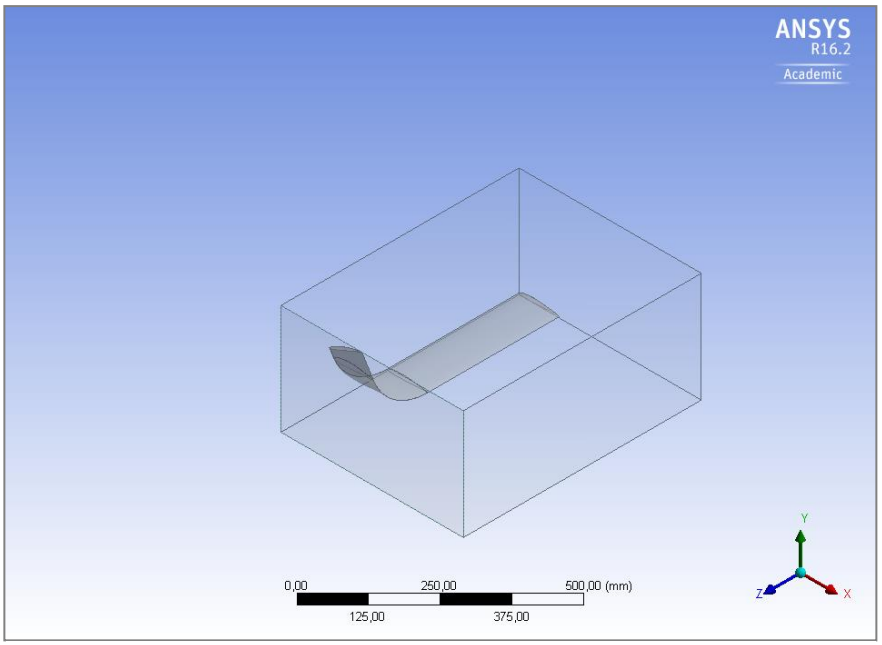

Figure 23. Geometry after generating the Enclosure.

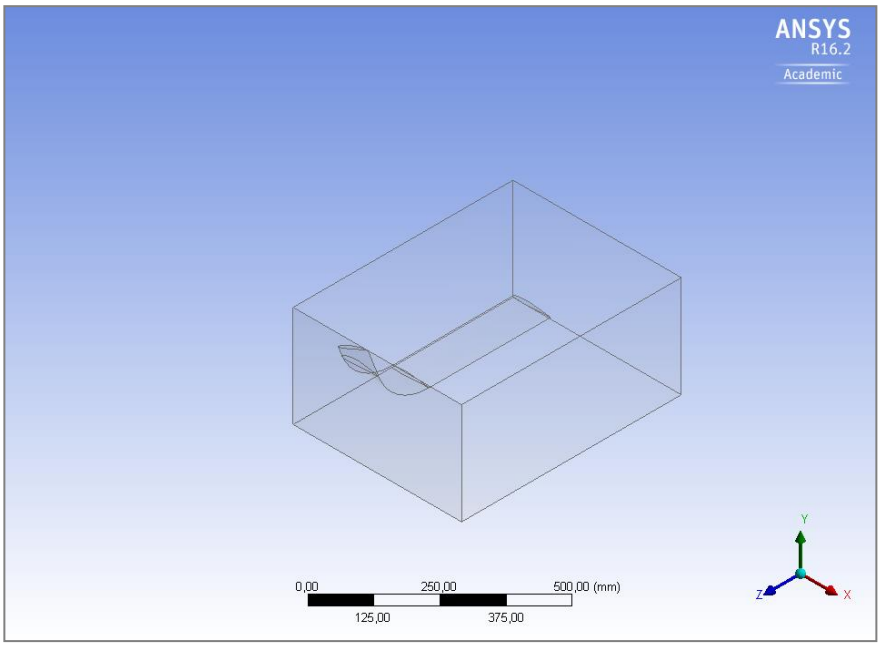

Figure 24. Final geometry after applying the Boolean operator.

ETSEIB

7.3. Meshing stage.

When in meshing mode, ANSYS functions as a robust, unstructured grid generation program that can handle grids of virtually unlimited size and complexity, consisting of tetrahedral, hexahedral, prismatic, or pyramidal cells.

It is important to remark that, when generating the mesh, it was necessary to find a balaced situation between velocity and pressure. The more accurate the mesh was, the more time would be recquired. Without overlooking the relevance of a good mesh, a meshig process that recquired too much time would have been counterproductive. Therefore, the desired equilibrium between velocity and pressure lied in selecting the adequeate mixture of a dense mesh and a lighter one.

- **Dense mesh:** the main advantage of a very dense mesh was that it offered a great accurancy in terms of calculation and results. However, it could take a very long time to obtain the final results, and this sluggish process could even block the computer or not reach a converged result.
- **Light mesh:** a lighter mesh can display the final results in an almost instantaneous way. However, these could probably differ very much from the reality, and they would be very far from the accurancy given by a more dense mesh.

Therefore, the mesh that was considered to be most suitable for this project was the one whose residual results were smaller that $1 \cdot 10^{-3}$.

Given that the design into which this project focuses is a 3D object, the complete mesh does not need to be particularly small and precise, but only certain parts of the geometry. A posterior refinement was executed, so that the results may be more accurate and realistic. Also, the element size of the entire geometry, as well as the edges, was specified:

- **Body sizing:** it is done by selecting the entire rectangular body – enclosure – and specifying the general meshing size.

  Type: Element size.

  Size: 1e-2 m

- **Edge sizing:** it is done by selecting only the edges of the inner empty body – where the E211 was before the *Boolean* operation was carried out – and specifying the meshing size, which will be inferior than that of the body sizing. This step is quite delicate since, as it has been stated, it is an inner geometry, which implies that, in order to see the profile, it will be necessary cut sections to see the profile.

  Type: number of divisions.

  Number of divisions: 500.

  Behavior: Soft.

Figures 25 and 26 illustrate some stages of the meshing process.

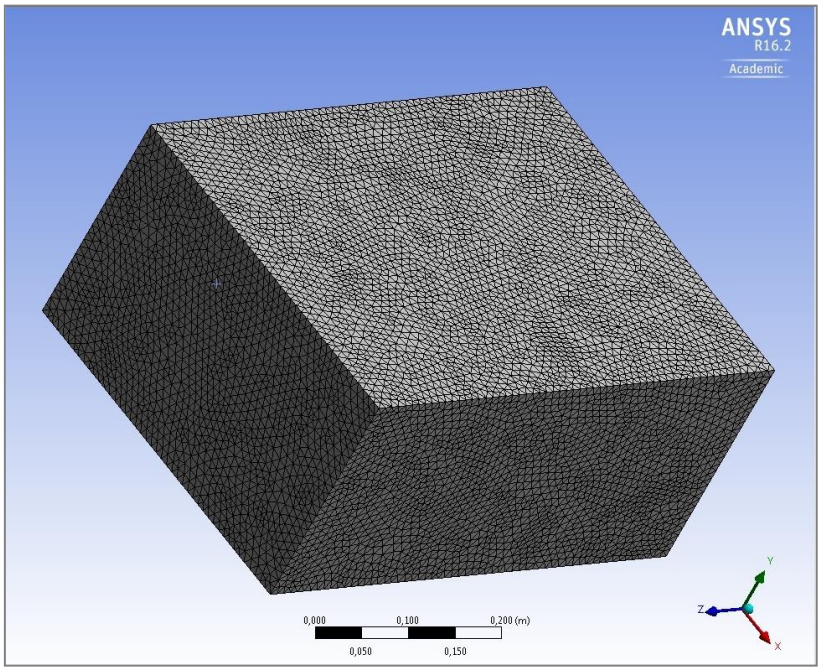

Figure 25. Final meshing of the entire body.

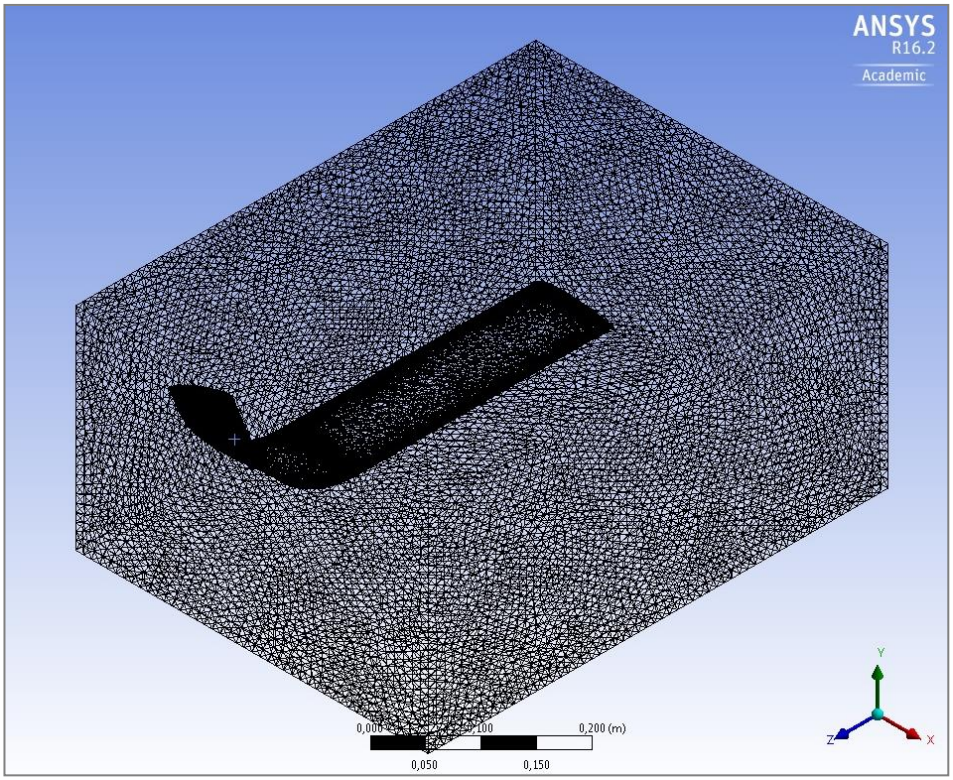

Figure 26. The hydrofoil after applying both Body and Edge Sizing.

These figures depict the final mesh of the blended winglet geometry. It is important to mention that some problems were faced when trying to mesh those geometries that included some sort of rounded face (o dome), since ANSYS Mesh Editor seem to have some difficulties with those type of geometries.

Therefore, the final mesh was (Figure 28) :

Relevance center: Fine.

Smoothing: High.

Transition: Slow.

Inflation: Smooth Transition

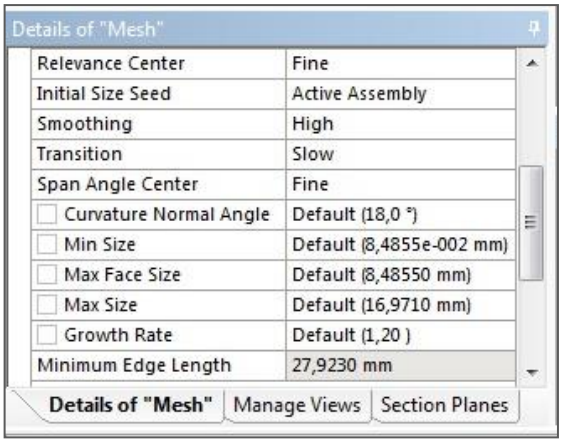

Figure 27. Final setting of the selected Mesh.

(ratio: 0,77, max layers: 5, Growth Rate: 1,2).

It was of utter importance to refine the mesh in those areas that are to be studied, since this allows the results to be more accurate and near to reality.

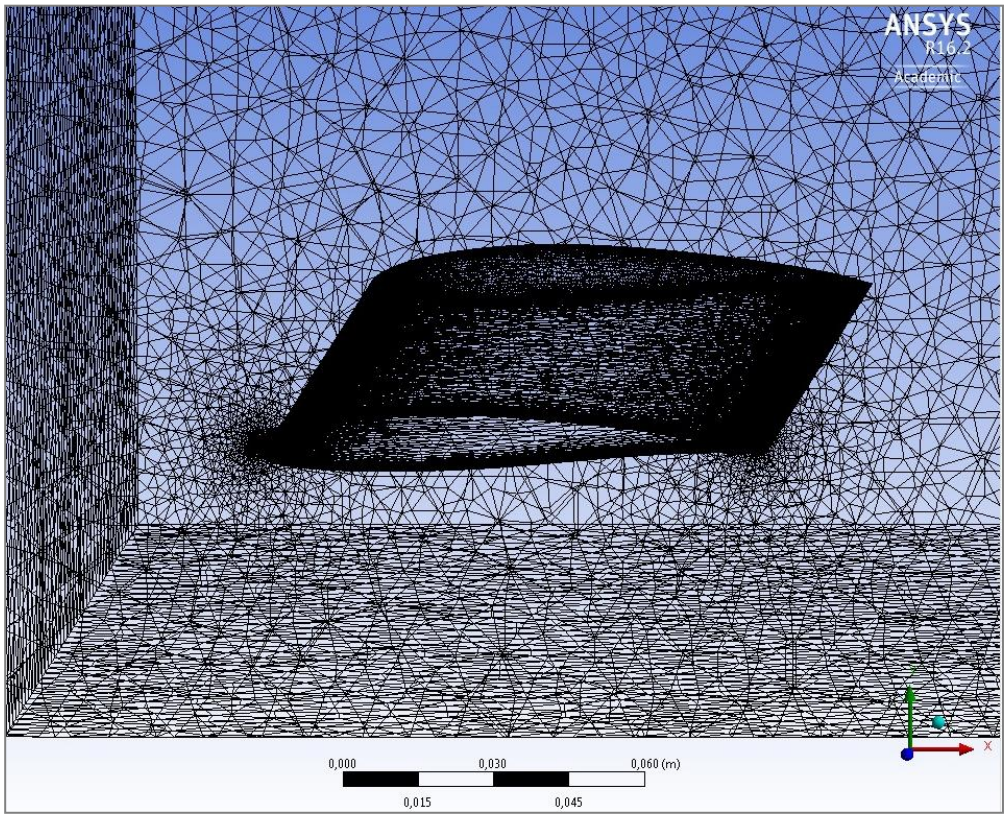

Figure 28. A cut off view of the hydrofoil once both Body and Edge Sizing were applied.

Finally, the last step was to select the diverse faces of the body and name them, so that they would be correctly identified by the Solver in the next stage. Therefore, the frontal face of the body – that which corresponds with the leading edge – was named INLET VELOCITY, which is where the water flow impacted first. The rear face – corresponding to the trailing edge – was called OUTPUT PRESSURE; the two lateral faces were named *Symmetries*,

since the flow passed through the body in a way that was the same for both of them; and, the upper and lower faces were called *Walls*. Finally, the contours of the E211+wingelt were called $hydro_i$, since these were the sections of the geometry that interacted with the fluid, and served to calculate both drag and lift. Annex A includes a deeper insight on the meshing process.

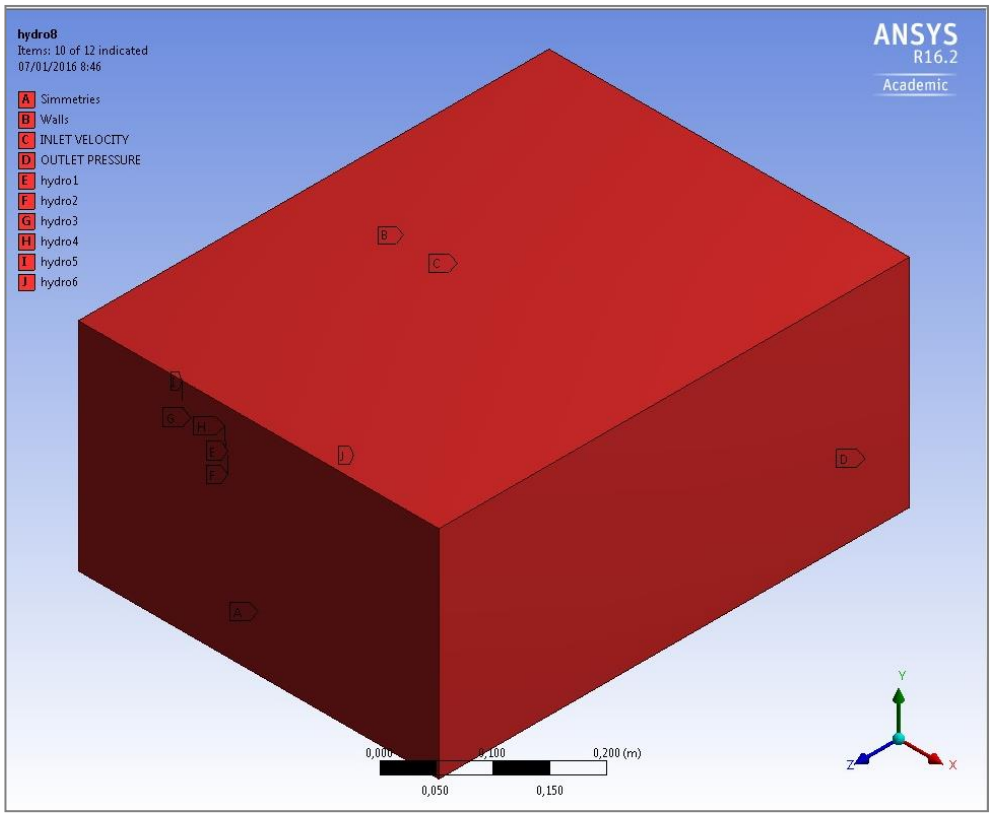

Figure 29. Body with the created sections once named.

7.4. Solver.

Once the mesh had been properly specified, it was necessary to set the conditions into which the simulation took place.

First, after importing the meshed geometry to the Solver, it was important to specify the model that would be employed to analyze the profile. As it has been previously stated, the selected model was the **Shear-Stress Transport (SST)**, since it blended the robust and accurate formulation of the *k-ω model*, and the freestream independence of *k-ε model*. In order to be able to specify the temperature of the flowing water, it was necessary to active the *Energy* option as well. Right after that, it was necessary to select water – liquid as a fluid, since the predetermined material is air. This had also to be considered when setting the Cell Zone Conditions.

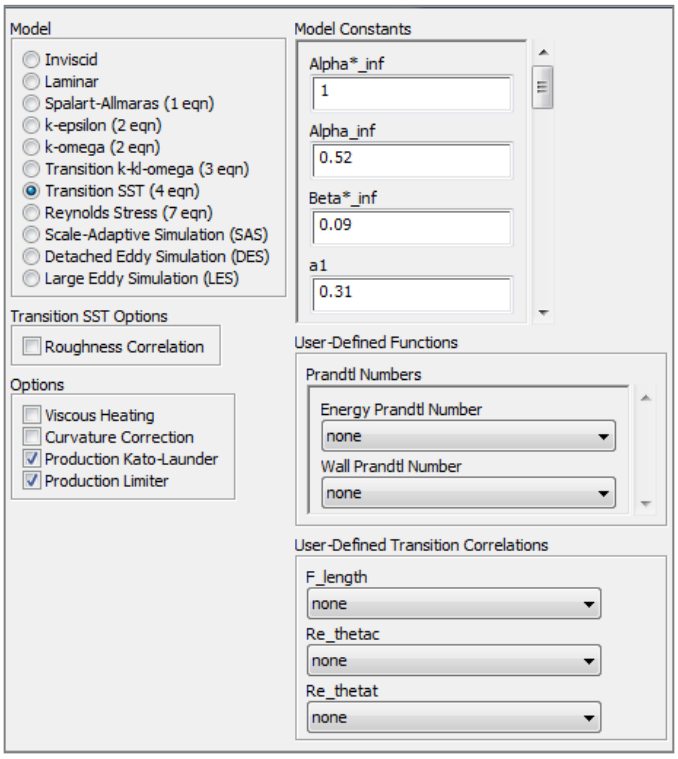

Figure 30. Panel to select the SST model.

Second, the Boundary Conditions had to be specified. Here, the INLET VELOCITY had to present a velocity of 12 m/s, and a temperature of 289 K (16ºC). Considering that the SST model is used, the Inlet Turbulence Levels had to be addressed too. Given that the turbulence intensity specified at an inlet can decay quite rapidly, it is advised to have relatively low inlet viscosity ratio (that is, 1 – 10), since it is estimated that at the leading edge of the hydrofoil,

the turbulence intensity will have decayed to the desired value. In the OUTLET PRESSURE, the gauge pressure was set at 0 Pa. The rest of the faces already appeared specified; Symmetries referred to the lateral faces, while Wall referred to both the upper and lower faces, and the hydro1 and hydro2 of the E211.

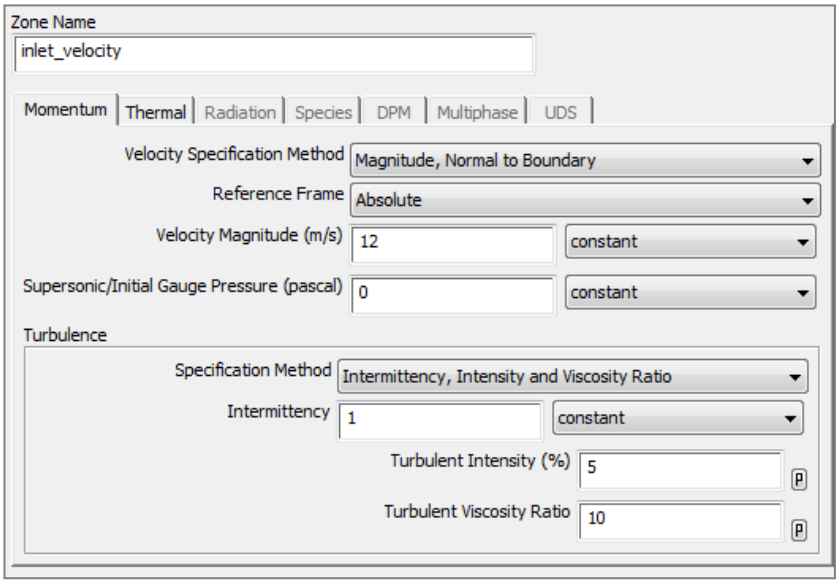

Figure 31. Setting the Inlet Velocity Boundary Conditions.

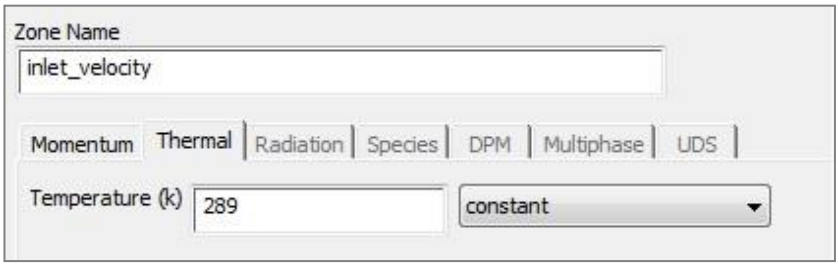

Figure 32. Stating the temperature at 289 K (16ºC).

Finally, when setting the Reference Values, it was important to set *compute from* as INLET VEOCITY, so that the water-liquid properties were automatically specified. Once all these characteristics had been set, time had come to move to the Solution section. There, in order to analyze the lift and the drag generated by the profile, it was necessary to add to

Monitors, and select the print, plot and write options so that the two coefficients appear in the analysis. Then, the solution had to be initialized, which required to set the *commute from* option to INLET VELOCITY; and finally, set the number of iteration to 1000 and start the calculation.

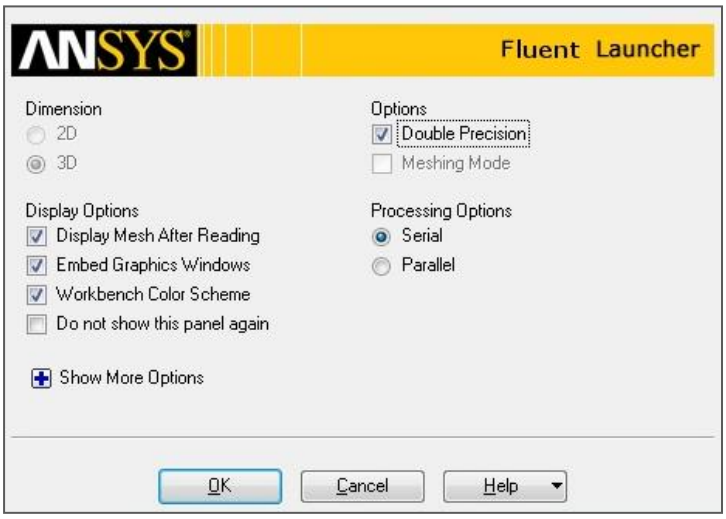

Figure 33. Initial settings of ANSYS Fluent.

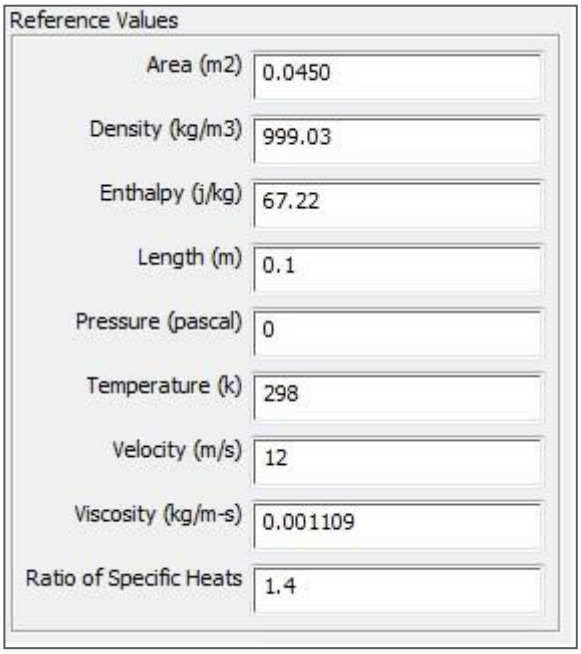

Figure 34. Reference values of the simulation.

8. Results.

The main objective of this analysis was to study the effect that the adding of wingtip devices had on the reduction of induced drag.

The first concept to consider was the induced drag present in the E211 naked model. Using the equation 7, detailed in section 6.3, and equation 8 induced drag can be calculated:

$$C_{Di} = \frac{C_L^2}{\pi \cdot AR \cdot e_0} \qquad \textbf{(eq. 7)}$$

$$D_i = \frac{1}{2} \cdot \rho \cdot v^2 \cdot S \cdot C_{Di} \qquad \textbf{(eq. 8)}$$

C_{Di} Induced Drag.

C_L Lift coefficient.

AR Aspect ratio.

e_0 Oswald efficiency number.

v Velocity of the fluid.

S Area of the hydrofoil.

ρ 999.03 kg/

$$C_{Di} = \frac{C_L^2}{\pi \cdot AR \cdot e_0} = \frac{0{,}43^2}{\pi \cdot 3{,}75 \cdot 0{,}76^*} = 0{,}0206$$

$$D_i = \frac{1}{2} \cdot \rho \cdot v^2 \cdot S \cdot C_{Di} = 0{,}5 \cdot 999{,}03 \cdot 12^2 \cdot 0{,}0375 \cdot 0{,}0206 = 55{,}57\ N$$

* For relatively small AR, e_0 is comprised between 0,7 and 0,85. Therefore, it has been considered that e_0 = (0,7 + 0,85)/2 = 0,76 (aprox.).

Therefore, in order to reduce drag, it was necessary to fulfill the following conditions:

$$C_{Di}{}^{Winglet} = \frac{C_L^{2\,winglet}}{\pi \cdot AR \cdot e_0} < 0{,}0206$$

$$\frac{C_L^{2\,winglet}}{AR} < 0{,}0206 \cdot \pi \cdot 0{,}76$$

$$\frac{C_L^{2\,winglet}}{AR} < 4{,}918$$

If, according to section 6.3, an AR = 7,1 is considered:

$$C_L^{2\,winglet} = 0{,}04918 \cdot 7{,}1$$

$$\boldsymbol{C_L^{2\,winglet} = 0{,}59}$$

In order to notice a reduction of induced drag it was necessary to have a lift coefficient of 0,59. Among the diverse candidates, both the blended winglet with bias tip and the blended winglet without bias tip were the ones that seemed to be the best options; also, their geometry had not presented any problems during the meshing process. However, after simulating the blended winglet without bias tip, together with a critical growth of the lift coefficient, an increase of the drag coefficient was also noticeable, which induced to think that the considered design was not the most adequate. Figures 34 and 35 depict the lift and drag coefficient that resulted from the simulation of the blended winglet with no bias tip.

	Lift Coefficient	Drag Coefficient
Blended winglet with no bias tip	0,670	0,0297

Therefore, the blended winglet with bias tip was tested. Finally, of the diverse designs considered and analyzed, the blended winglet with bias tip was the one whose lift coefficient was closest to this condition, presenting a value of 0,573 and a reduction of the drag coefficient.

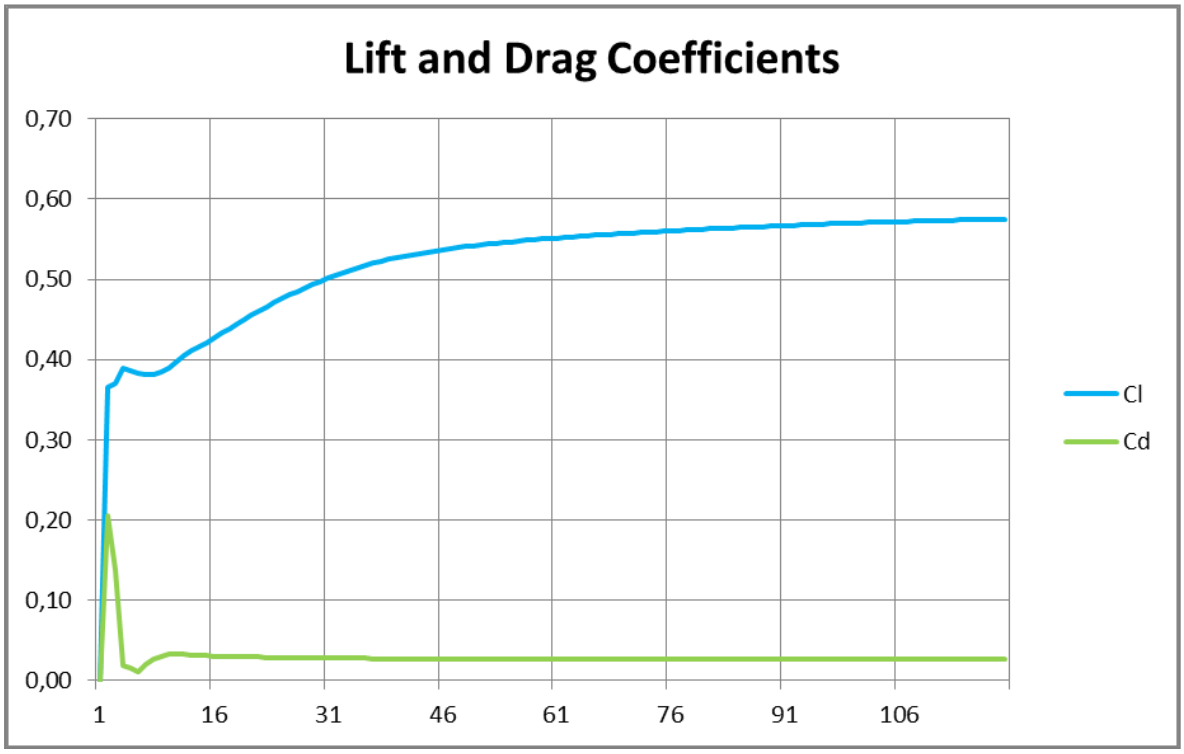

Figure 36. Graph of both Lift and Drag coefficient along every iteration.

	Previous values	Current Values
Lift Coefficient	0,43	0,573
Drag Coefficient	0,029	0,0273

Figure 35. Final values of both lift and drag coefficient.

Observing these results it can be easily deduced that, for a slight reduction of drag, a substantial increase of lift coefficient was produced. This is explained by the fact that a considerable part of the lift coefficient was employed to counteract the harming effect that induced drag had on the hydrofoil. Now, if equations are recalculated using this value, the following results are obtained:

$$C_{Di}{}^{Winglet} = \frac{C_L^{2\,winglet}}{\pi \cdot AR \cdot e_0} = \mathbf{0{,}0197 < 0{,}0206}$$

$$D_i = \frac{1}{2} \cdot \rho \cdot v^2 \cdot S \cdot C_{Di} = \mathbf{50{,}30\ N < 55{,}56N}$$

As values indicate, there was a reduction of induced drag which simultaneously resulted in an increase of lift. The gain in lift is justified precisely because the addition of a winglet helped produce aerodynamic forces that diverted the flow of air from the tip vortex; that is, winglets still produced induced drag, but a much weaker one. Therefore, water resistance was lowered, thus allowing lift to achieve higher values. Figure 37 depicts the Scaled Residuals that resulted from the final simulation with ANSYS Fluent. It can be noticed that they reach values of $1 \cdot 10^{-3}$; therefore, they were considered acceptable.

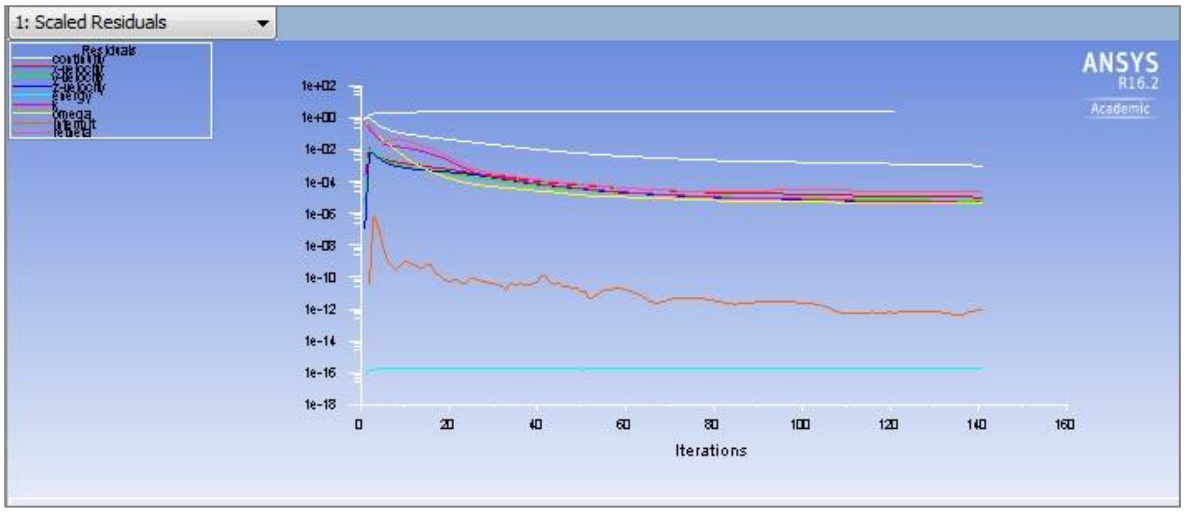

Figure 37. Scaled Residuals resulting from the final simulation.

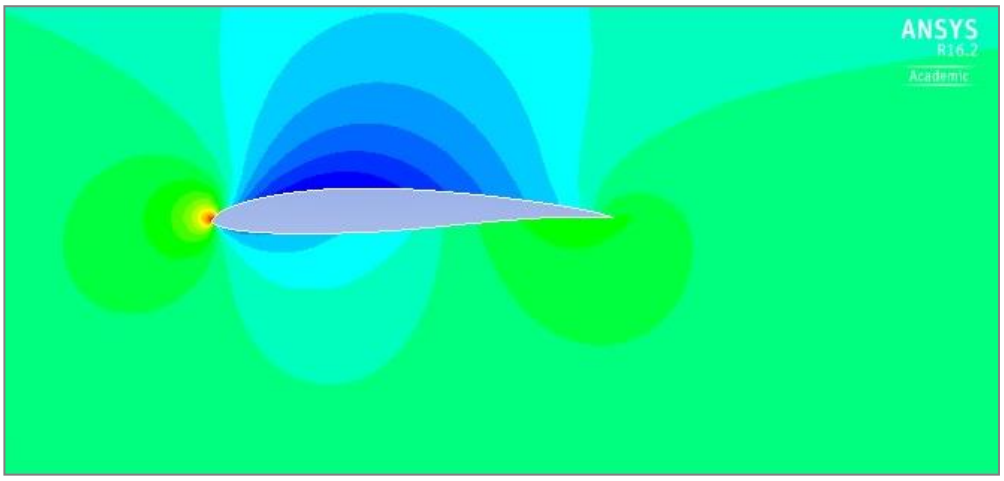

Figure 38. Static pressure distribution of the E211 profile.

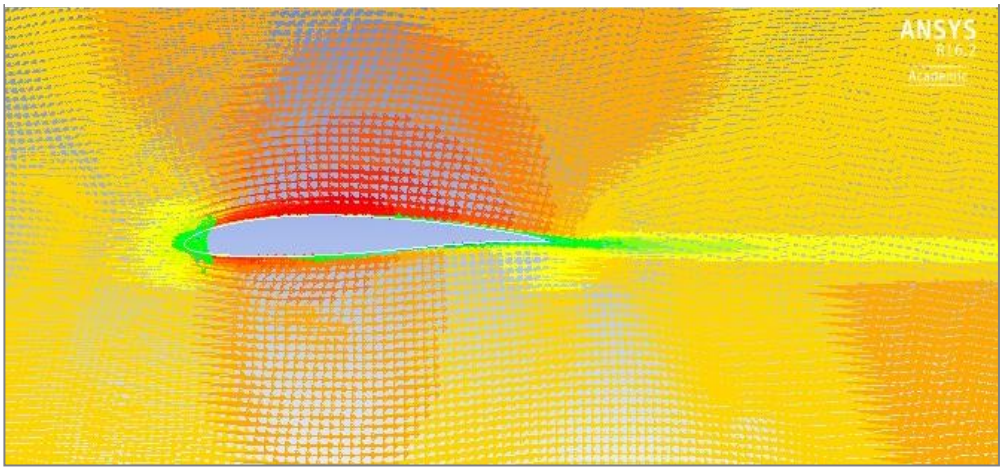

Figure 39. Velocity vector distribution of the E211 profile.

Finally, Figures 38 and 39 depict the static pressure distribution (contour) and the velocity vector distribution of the E211 profile before the simulation had been finished. As it can be observed, there was a stagnation point right in the outer point of the leading edge, which corresponded to the fact that static pressure reached its highest value at the same point. Also, the existing gradient of pressure can be perceived. This gradient of pressure caused the presence of high values of induced drag which were eventually reduced by the addition of the blended winglet. For the simulations results of the other geometries see Annex A.

9. Cavitation.

Cavitation is defined as the process of formation of the vapor phase of a liquid when it is subjected to reduced pressures at constant ambient temperature. Therefore, a liquid is said to cavitate when vapor bubbles form and grow as a consequence of pressure reduction.

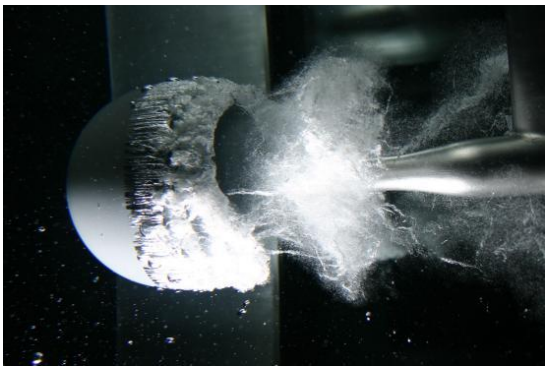

Figure 41. Collapsing bubble[(13)].

When the phase transition results from hydrodynamic pressure changes, a two-phase flow composed of liquid and vapor is called a *cavitating flow* [Phillip Eisenberg, 1950][(13)]. Given the situation that flow pressure reaches values under the vapor pressure of the liquid, its molecules immediately change into vapor state, forming the stated bubbles or cavities. These bubbles travel to sections where pressure values are higher and collapse; that is, vapor suddenly turns into liquid once again. This implosion causes erosion of the metal surface that originates this phenomenon, and it also gives rise to waves of expansion that travel through the fluid at near sonic velocities. These waves can eventually dissipate or they can clash against a body; if this body is the one that generated the phenomenon, they cause erosion and turn the surface of the body into a section where pressure loss is higher, and therefore causes even more cavitation. If the collapsed bubbles are located near a solid wall, the forces that appear generate extremely high local pressures that harm the surface.

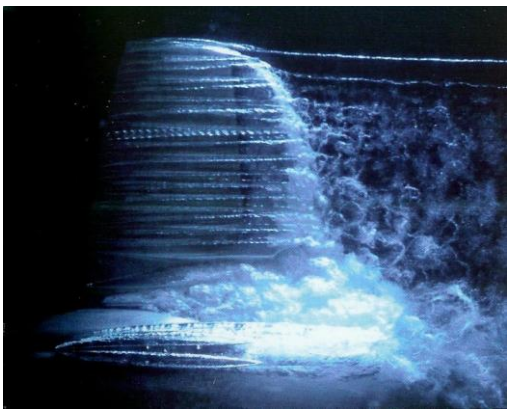

Figure 40. Cavitation in a hydrofoil[(13)].

Depending on the composition of the surface, the body could oxidize and eventually, disintegrate. In addition, these bubbles are generally followed by noise and vibration, which generates the effect of sand hitting the surface.

9.1. Flow about Hydrofoils.

Studying the case of a thick, symmetrical hydrofoil, the flow speed is increased until cavitation occurs. It first starts at the intersection of the strut and hydrofoil, where the presence of the strut causes a greater pressure reduction than elsewhere of the foil. The bubbles collapse as they are swept downstream into the higher-pressure region near the trailing edge.

Figure 42. Cavitation in a hydrofoil[13].

9.2. Effects of the cavitation.

Here, some of the main effects that may result from the appearance of cavitation on a hydrofoil are presented [Phillip Eisenberg, 1950][13].:

- The profile can be seriously harmed, since the high pressures that the bubbles exert when they collapse can cause the material failure.
- It decreases lift and increases drag.

- The surrounding flow can become unstable.
- Noise and vibrations are caused by the collapsing bubbles.

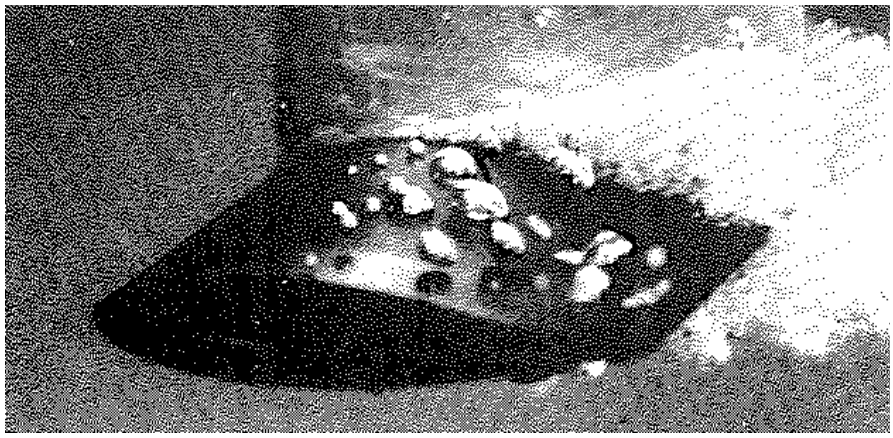

Figure 43. Collapsing bubbles around the upper Surface of a hydrofoil[(13)].

9.3. How to avoid cavitation.

Cavitation occurs to various degrees in all types of fluid handling equipment, including propellers, pumps, large turbines and hydrofoils. Given its harmful nature, it is imperative to assure that the phenomenon does not manifest by employing several methods.

One of these methods consists in increasing the gradient of static pressure between the fluid and its vapor pressure at a given temperature. This can be done by increasing the temperature of the fluid or the pressure of the entire system. However, these factors are not always controllable, so it is highly advisable to search for another more reliable method; like the use of cavitation resistant surfaces, or coatings [Ryan Sollars and others, 2011][(14)].

This last option remains one of the most economical ways to control cavitation, and there is a vast extension of materials that can be used. For instance, selecting a wear surfacing alloy such as austenitic stainless steel has been a traditional solution for many years. With severe

cavitational wear, the use of high carbon, cobalt base alloys with relatively high hardness and corrosion resistance has also been used. However, these are more crack-sensitive and relatively quite expensive.

Still, over the last few years, new important discoveries have been achieved. Hattori Shuji and Itoh Takamoto, from the School of Engineering in the University of Fukui, in their article[(15)], stated that the several cavitation erosion tests carried out for plastics – such as epoxy resin, polypropylene, high-density polyethylene and polyamide 66 – concluded that their cavitation erosion resistance ranged from between half and 30 times that of carbon steel alloys. Therefore, impact loads on plastic surfaces were lower than those of metals.

Simultaneously, even though natural rubber is a proven wear and corrosion protection material, its restricted reparability makes it not a generally good recommendation. There are, however, several elastomeric materials systems – like the MetaLine Series – that combine rubber quality features and make it possible to apply spryable elastomer protection coatings directly on-site. Also, these sort of materials have the advantage that, contrary to natural rubber, they are based on a special PUR-Elastomer technology that does not require vulcanization [Metaline®, 2012][(16)].

These new materials are abrasion/erosion resistant, permanently elastic, shock absorbing and cavitation minimizers. Annex B provides the detailed technical data of these spray elastomers.

Typically, cavitation resistance coatings are used in larger devices like turbines, and they may have no noticeable result in small hydrofoils attached to windsurfing boards. Still, these recent discoveries may give birth to a new branch of cavitation resistance materials

that might substantially less expensive and consistently more effective.

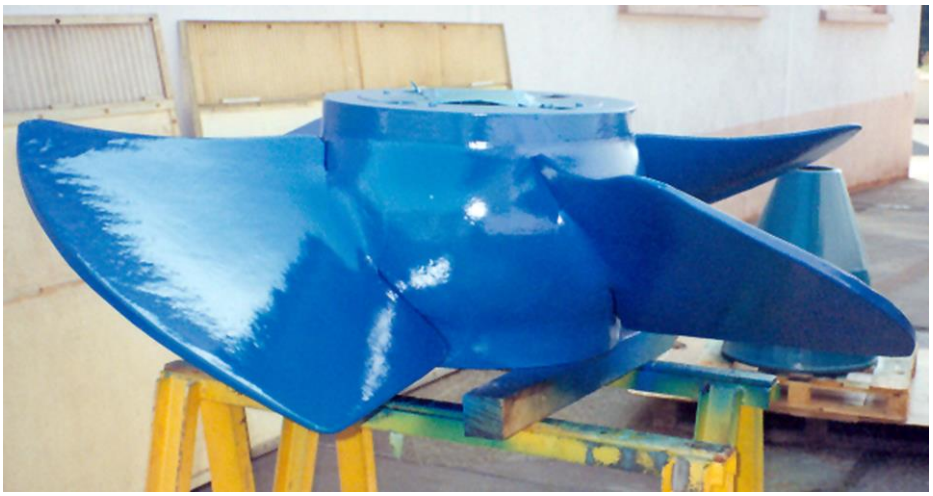

Figure 44. An example of cavitation resistance elastomeric coating[16].

Figure 39 depicts an example of cavitation resistance coatings, showing a propulsion system of a watercraft.

9.4. Cavitation in ANSYS Fluent.

After the simulation of the diverse profiles, the following graph of pressures has been obtained.

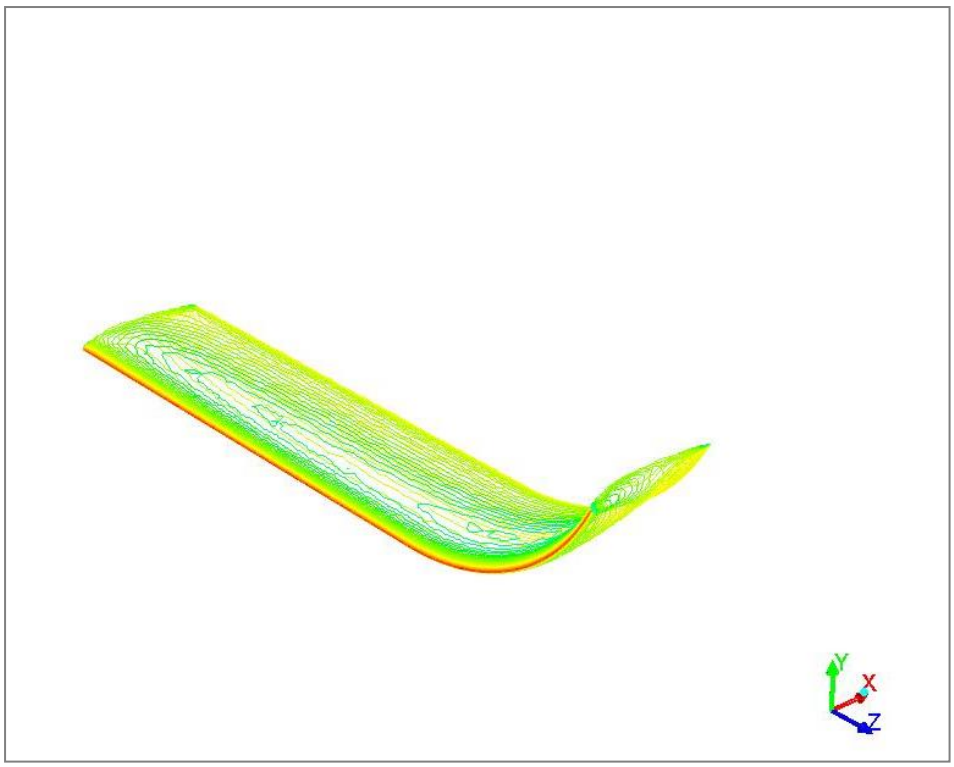

Figure 45. Static pressure distribution in the final selected model.

In order to detect whether the selected design cavitates or not, it was necessary to consider the following conditions.

Cavitation occurs when the fluid pressure reaches values under the vapor pressure, that is:

$$P_{min} \leq P_{vap}$$

$$P_{vap} = 1818{,}8\ Pa$$

This causes bubbles to appear and eventually collapse, provoking erosion and degradation of the surface of the hydrofoil.

Hence, it is essential to verify that this condition did not happen.

As Figures 44 and 45 depict, both maximum and minimum pressure values where:

$$P_{max} = 72661{,}26\ Pa$$

$$P_{min} = -66779{,}83\ Pa$$

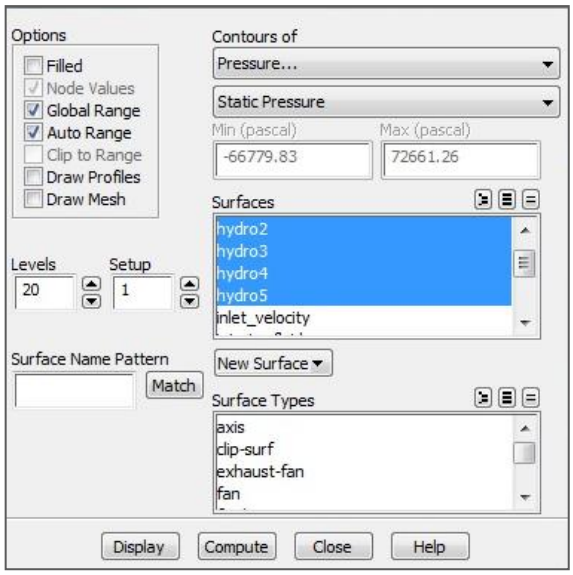

Figure 46. Minimum and máximum pressure.

In consequence, according to this:

$$P_{abs} = P_{rel} + P_{atm}$$

$$P_{abs} = 101325\ Pa$$

$$P_{max} = 72661{,}26 + 101325 = 173986{,}26\ Pa$$

$$P_{min} = -66779{,}83\ Pa + 101325 = \mathbf{34545{,}17\ Pa}$$

$$\mathbf{34545{,}17\ Pa} > \mathbf{1818{,}8\ Pa}$$

$$P_{min} > P_{vap}$$

Therefore, the fluid pressure is higher than the vapor pressure, which indicates that no cavitation phenomenon occurs during the analyzed experimentation.

Besides analyzing the Static Pressure, it was also interesting to give a look to the velocity distribution (Figure 46).

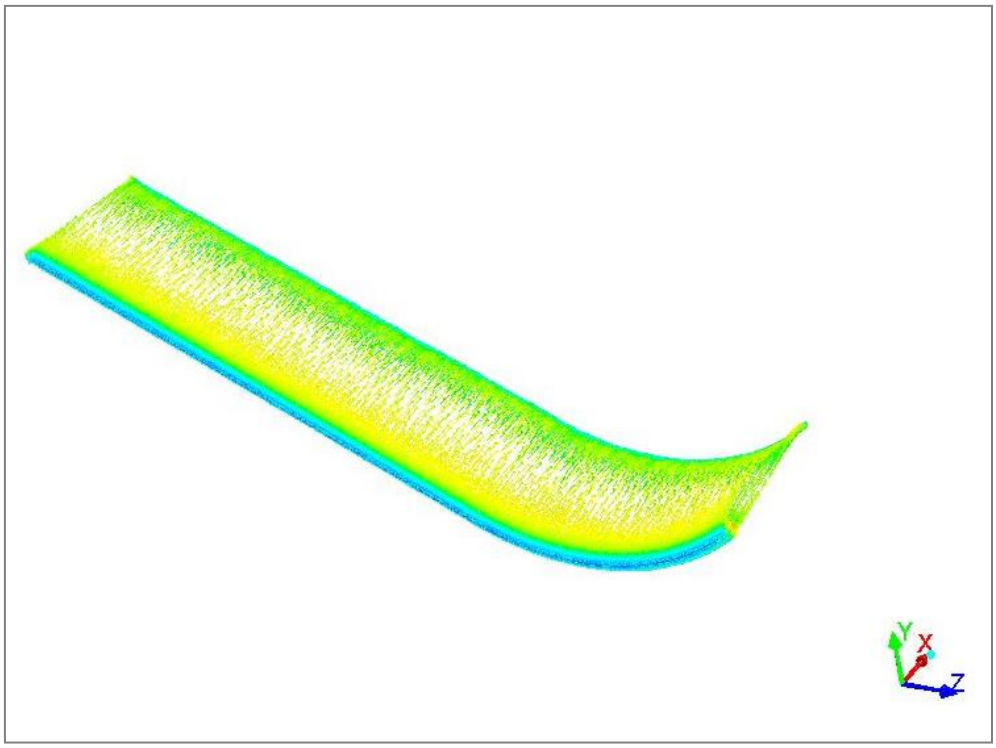

Figure 47. Vector velocity distribution along the hydrofoil.

It is easy to notice that the minimum velocity (point of stagnation) appeared precisely were the maximum pressure was; and that it increases along the surface upper surface of the hydrofoil, just like pressure decreases. This goes in accord to what had been stated at the beginning of the project: that there is a gradient of pressure (high pressure in the lower section, low pressure in the upper section) that originates a circulation of the flow from the lower section to the upper section, thus generating wingtip vortices.

However, when working with the SST model, it is interesting to see the Turbulence Dissipation, which could help to the understanding of the behavior of the flow in these new conditions. This can be done by analyzing the Production Turbulent Kinetic Energy and Turbulence Intensity (Figures 47 and 48).

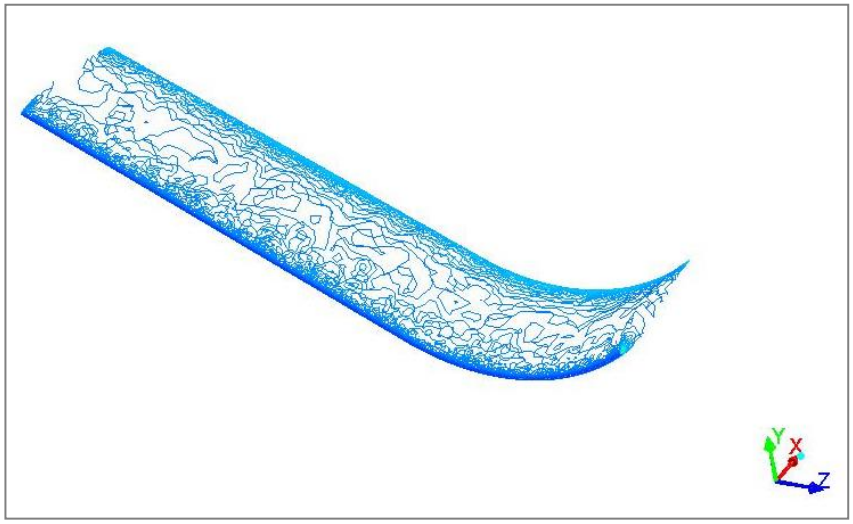

Figure 48. Turbulent Kinetic Energy Distribution.

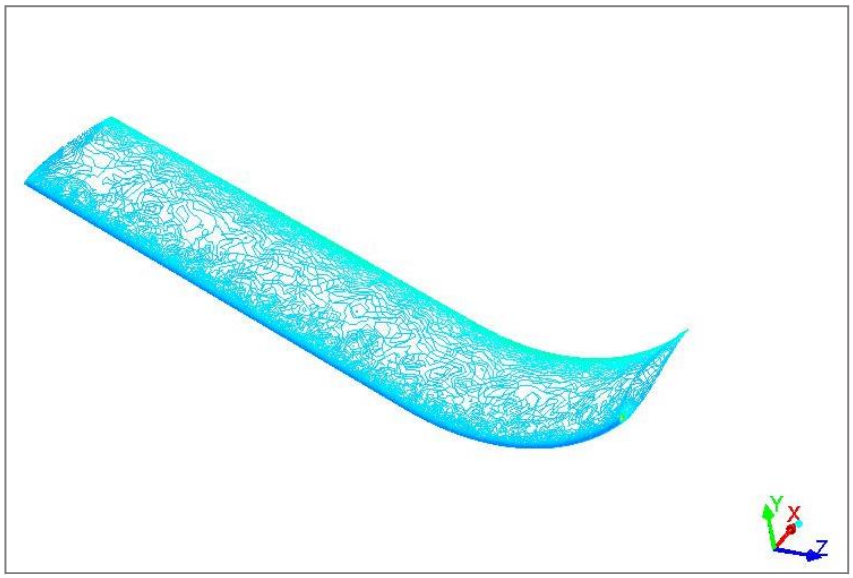

Figure 49. Turbulence Intensity Distribution.

As both Figures depict, the front area of the hydrofoil presents very low values of turbulence, and it is in the rear section that Turbulence started to appear. Also, it can be

noticed that there is a slight amount of turbulence right in the front upper point of the winglet, which hints the possibility of a future betterment of the design.

10. Model construction.

According to Frank M. White[17], most practical fluid flow problems are too complex, both geometrically and physically to be solved analytically. They must be tested by experiment or approximated by computational fluid dynamics (CFD). Dimensional analysis and Similarity is a method employed for reducing the number and the complexity of experimental variables that affect a given physical phenomenon by using some sort of compact technique that would allow the correct construction of a model.

Despite the many advantages of numerical simulations, the most accurate way to analyze the behavior of a flow around a given design is to build a model and experiment upon it. However, bearing in mind the academic nature of this project, the available economic resources are substantially limited and the construction of the model has been forced to be merely hypothetical. Therefore, a brief study of the most adequate material to build the model has been carried out.

10.1. Windsurfing board and hydrofoil materials diversity.

Windsurfing boards are generally rated in terms of volume and length. Volume refers to how much flotation the board offers; meaning that high volume and long lengths suit light wind sailing, while low volume and short boards are for high-wind performance. Given that the width = 0,100 m of the windsurfing board studied in this project is based upon the one that was used in *Hidrodinàmica i Aplicació dels Hydrofoils al Windsurf*, and that the velocity of the fluid was 12m/s, it has been

Figure 50. Example of a longboard for windsurfing[18].

considered that the studied model was a *longboard*, thus suiting the light wind conditions. Figure 49 depicts an example of a longboard for windsurfing.

Generally speaking, a windsurfing board – as well as the attached hydrofoil – can be made of Expanded Polystyrene Foam (EPS), Epoxy, Fiberglass or PVC, although in some cases boards can be made of a mixture of these materials along with many others. For a deeper insight of the diverse materials used to build windsurfing boards and their hydrofoils, see Annex B.

Still, the most common materials are Fiberglass and Epoxy. Fiberglass boards are shapely and fast, and substantially more expensive. They are often used for high-wind boards, but they are quite easy to dent. While Epoxy boards have the same construction as fiberglass boards, are less expensive, and result in a very responsive boards. These, however, are usually used for light wind sailing. Therefore, the latter seems to suit better the conditions of the current project.

10.2. Why Epoxy?

Epoxy popularity grew in 2006 due to an increasing necessity of more affordable and equally efficient boards given the sudden high level of popularity that windsurfing reached at that time. Makers of epoxy windsurfing boards proclaimed their lightweight construction and ability to take more punishment than fiberglass boards. Many companies producing epoxy windsurfing boards – such as Surftech, Firewire and Resin8 – advertised these boards as being more durable and more buoyant than traditional fiberglass boards. Epoxy boards have more plastic-looking finish, are more impact resistant and, what is more important in the current case, they are substantially less expensive than fiberglass boards.

Also, a study carried out by Denis Gallagher[18] hinted that the epoxy board seemed to be able to handle the impact resistance much better that the fiberglass board, and that they were easier to paddle, catch a wave and turn than the latter. Still, it seemed that the most proficient surfers that participated in this study found a slight loss of control when carrying out more radical moves. However, the final conclusions were that, in general terms, epoxy board provided an equally efficient choice for building windsurfing boards – and hydrofoils – and offered much affordable prices. Therefore, considering that the current study worked at speeds of 12 m/s – which can be considered light wind sailing conditions –, that the water flow direction was always perpendicular to the leading edge of the hydrofoil; that is, no radical moves are to be expected, and that the available economic resources are substantially limited; the final selected material was **Epoxy**.

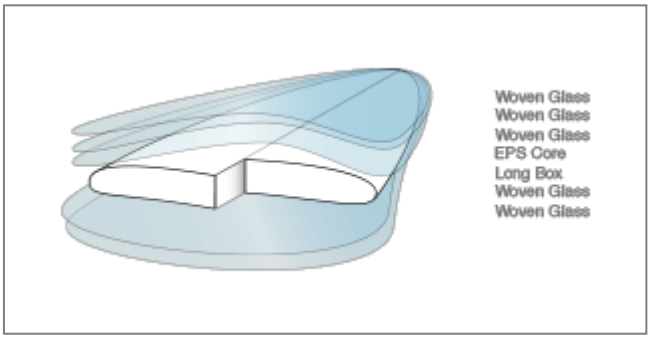

Figure 51. The X-1 Epoxy model: an example of an Epoxy windsurfing board[21].

10.3. BioFoam: a brand new option.

Yet, another new material has recently appeared as a result from the quest for the ultimate sustainable windsurfing board material: BioFoam surf blanks by HomeBlown. These boards have close to 50% of their core ingredients sourced from plan-based agriculture product, and it is suggested that BioFoam production results in 36% less global warming emissions and a 61% reduction in non-renewable energy use.

This revolutionary foam makes the windsurfing boards stronger, lighter, and hydrophobic while simultaneously being 36% more sustainable. Therefore, BioFoam could perfectly be the object of a future research of better and more sustainable materials for building a windsurfing board model.

For a deeper insight on both Epoxy and BioFoam characteristics, see Annex B.

Figures depict an example of BioFoam processing, and a BioFoam board.

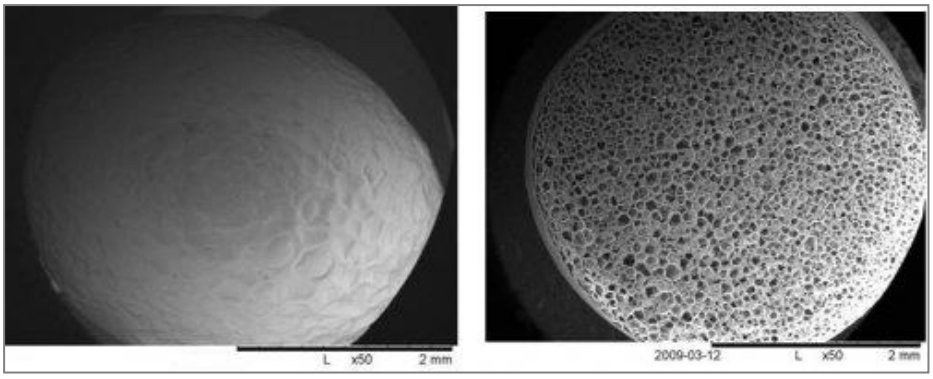

Figure 52. An example of BioFoam processing[19].

Figure 53. An example of a BioFoam board[19].

11. Environmental Impact.

When elaborating this project, some environmental aspects have been considered.

Bearing in mind that the aim of this project is none other than to reduce induced drag and therefore, increase lift; it is obvious that both conditions lead to a common effect, and that is the saving of energy and fuel, which eventually translates into a smaller carbon footprint. While it is true that building and attaching winglets may be slightly more costly than simply using the naked model, the environmental benefits that derive from their use are endless and completely worthy.

Figure 54. Environmentally friendly.

In the particular case of blended winglets, for instance, besides their many performance improvements, there is also a noticeable reduction in emissions and noise. Still, all these aspects refer to the general use of (blended) winglets. In this particular project, the studied craft is a windsurfing board, which is powered by a sail, so the energetic cost is practically non-existent. The reduction in fuel consumption would certainly play a more significant role were the watercraft be powered by some sort of engine.

It is also important to remark that this project is based upon numerical simulations, whose environmental impact and cost is near to insignificant compared to the physical construction of a model and its posterior experimentation. Numerical simulations have also avoided the use of not environmentally friendly materials.

In the case of the hypothetical construction and testing of a model of the windsurfing board – with its correspondent attached hydrofoil – the energetic and environmental cost, which can be understood in terms of carbon footprint, would have to be considered.

For example, it would be imperative to consider the extraction of raw materials, their processing, the manufacture of the board, the transportation, the shaping, the repair and maintenance, and the final disposal. The annual production of new surfboards – roughly 750,000 – creates around 220,000 Tons of CO_2. For instance, an average Polyester *Shortboard* has the carbon footprint of around 182 kg of CO_2.

Still, the trend for windsurfers to go green has become evident, and more friendly products are being demanded. As a response, in the early 80s Epoxy resins windsurfing boards appeared. Epoxy resin has about 75% fewer Volatile Organic Compounds (VOCs) that Polyester, and about 2/3 fewer VOCs are released into the atmosphere when it cures. Also, Epoxy resins can be cleaned up with organic citrus based cleansers rather than flammable and toxic acetone, and it can be derived from several types of plan resources, including sugar. In addition to less toxic, windsurfing boards using Epoxy resins maintain greater durability, which translates into a more environmentally friendly product.

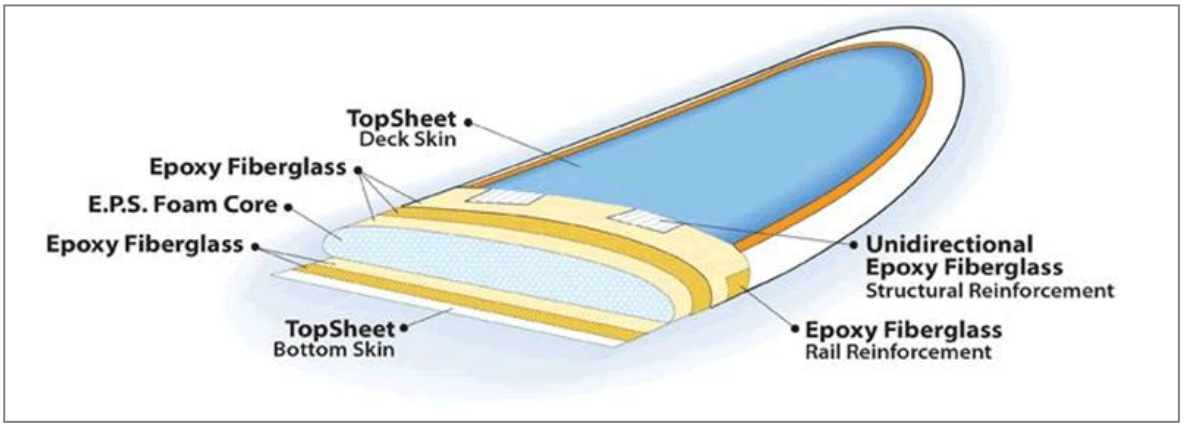

Figure 55. Example of an Epoxy board[18].

Therefore, the environmental impact of building a small model made of Epoxy resin would not be great. Still, there could be a much more environmentally friendly alternative, which would be using BioFoam to elaborate the model.

The most important gain of using BioFoam lays in the fact that during the growth of the sugar plants to produce lactide based PLA (which in the end will lead to moulded BioFoam), nett CO_2 is absorbed. On the average only 30 – 40% of the CO_2 will be emitted compared to the production of other polymers, which represents a reduction of 60 – 70%.

Figure 55 depicts the result of a comparative study carried out by BioFoam Synbra Group[19] in order to analyze the amount of CO_2 generated by the production of 1 ton of polymer production. As it can be observed, PLA lactide based (base for BioFoam) presents the lowest values.

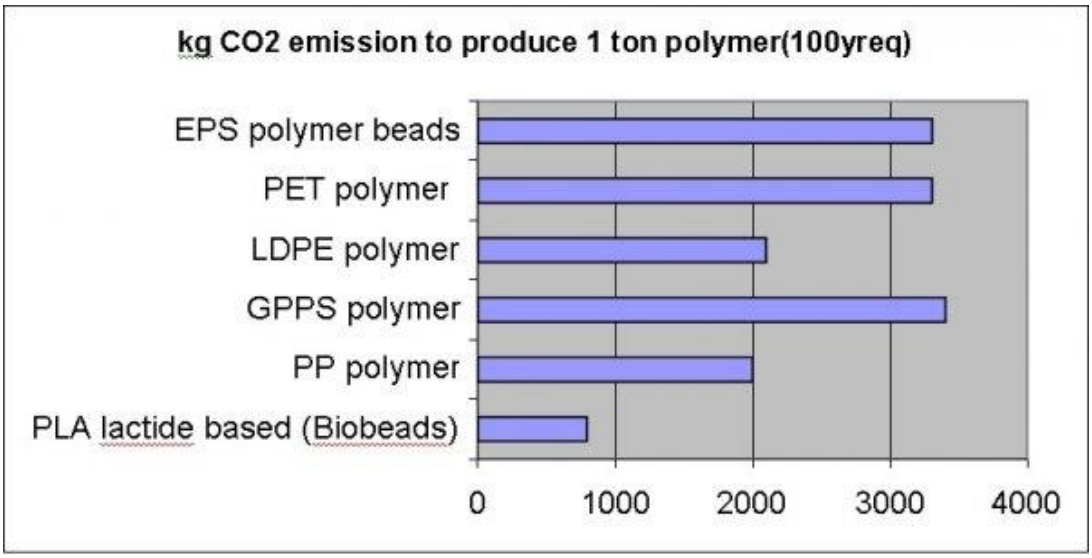

Figure 56. CO_2 emission arising from the production of 1 ton polymer production[19].

12. Economic viability.

A study of the economic viability has been produced in order to use it as a guideline in case this project ever reaches a stage where the construction of the E211 hydrofoil is desired. Every needed expense during the elaboration of this project has been included in this study.

Service	Quantity [h]	Price [€/h]	Cost [€]
Industrial Engineer	470	25	11750
ANSYS Student License	-	-	300
SolidWorks License	-	-	350
Microsoft Office License	-	-	120
Current Computer	-	-	1500
Administrative Tasks	-	-	125
		Total	**14145 €**

Total (without I.V.A)	14145 €
I.V.A (21%)	2970.45 €
Total cost with I.V.A (21%)	**17115.45 €**

In addition, Figure 43 depicts the costs distribution of the current project.

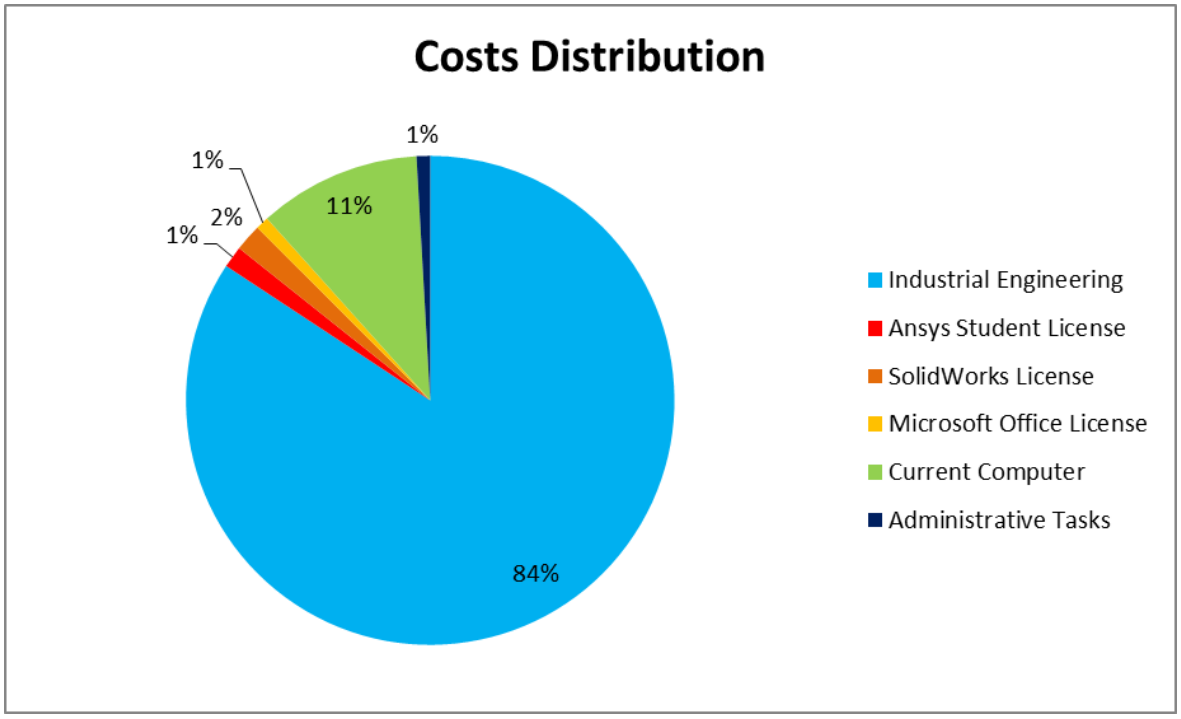

Figure 57. Graph illustrating costs distribution.

13. Timeline.

The general duration of a Final Year Dissertation is a four-month period; therefore, the timeline has been organized according to this period of time.

Within the project itself, there were different stages, each of which required different durations, as well as presenting different start and end dates. In order to illustrate these data in a clearer manner, a Gantt diagram has been done (Figure 59). In addition, a color-based code has been attached, so that the timeline is even easier to understand.

Color-based code	Stage	Total Duration
Yellow	Research	3
Blue	Experimentation Process	16
Green	Writing Process	10
Red	Oral Presentation	2

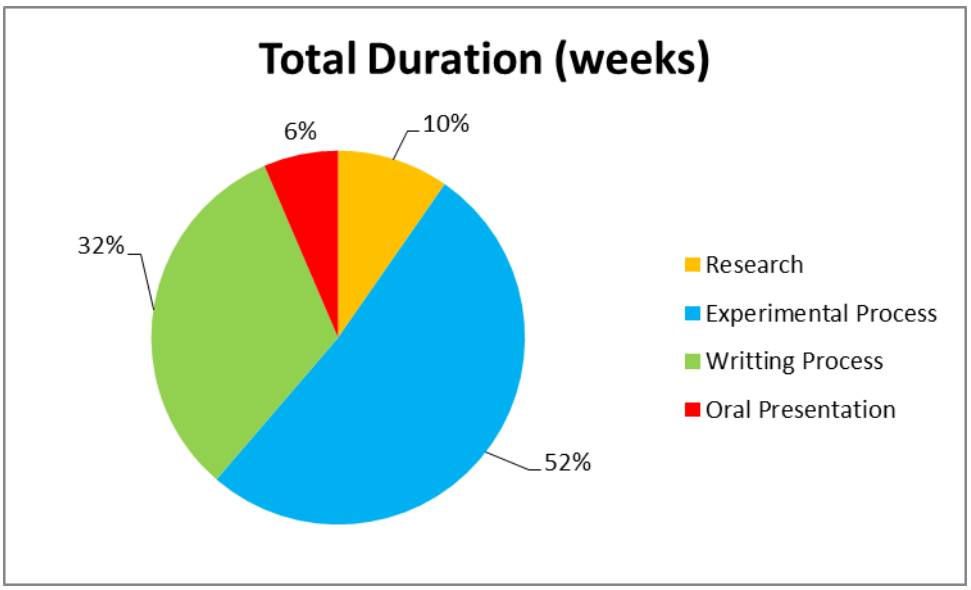

Figure 58. Graph illustrating the distribution of the total duration of the project.

Activity	Start	Length	Start date – End date
Research: E211 hydrofoil, previous project...	1	1	01/09/2015 – 07/09/2015
Research: Induced Drag, Winglets, cavitation…	1	2	01/09/2015 – 13/09/2015
Winglets selection process	1	2	01/09/2015 – 13/09/2015
Mathematical calculation of desired induced drag	3	2	14/09/2015 – 27/09/2015
Writing mathematical calculation section	5	1	25/09/2015 – 28/09/2015
Writing Introduction, abstract, objective….	5	1	25/09/2015 – 28/09/2015
SolidWorks modelling process	6	3	28/09/2015 – 18/10/2015
Simulations process	9	3	01/11/2015 – 15/11/2015
Comparision of results from different geometries	12	2	15/11/2015 – 29/11/2015
Selection of the final geometry	12	2	15/11/2015 – 29/11/2015
Results analysis and conclusion deduction	14	2	01/12/2015 – 12/12/2015
Writing modelling process, simulation process…	16	2	18/12/2015 – 31/12/2015
Writing cavitation, conclusions, annexes, review…	18	4	21/12/2015 – 07/01/2016
Oral presentation preparation	22	2	12/01/2016 – 28/01/2016
Oral presentation	23	1	28/01/2016

Figure 59. Gantt diagram depicting the duration of the project.

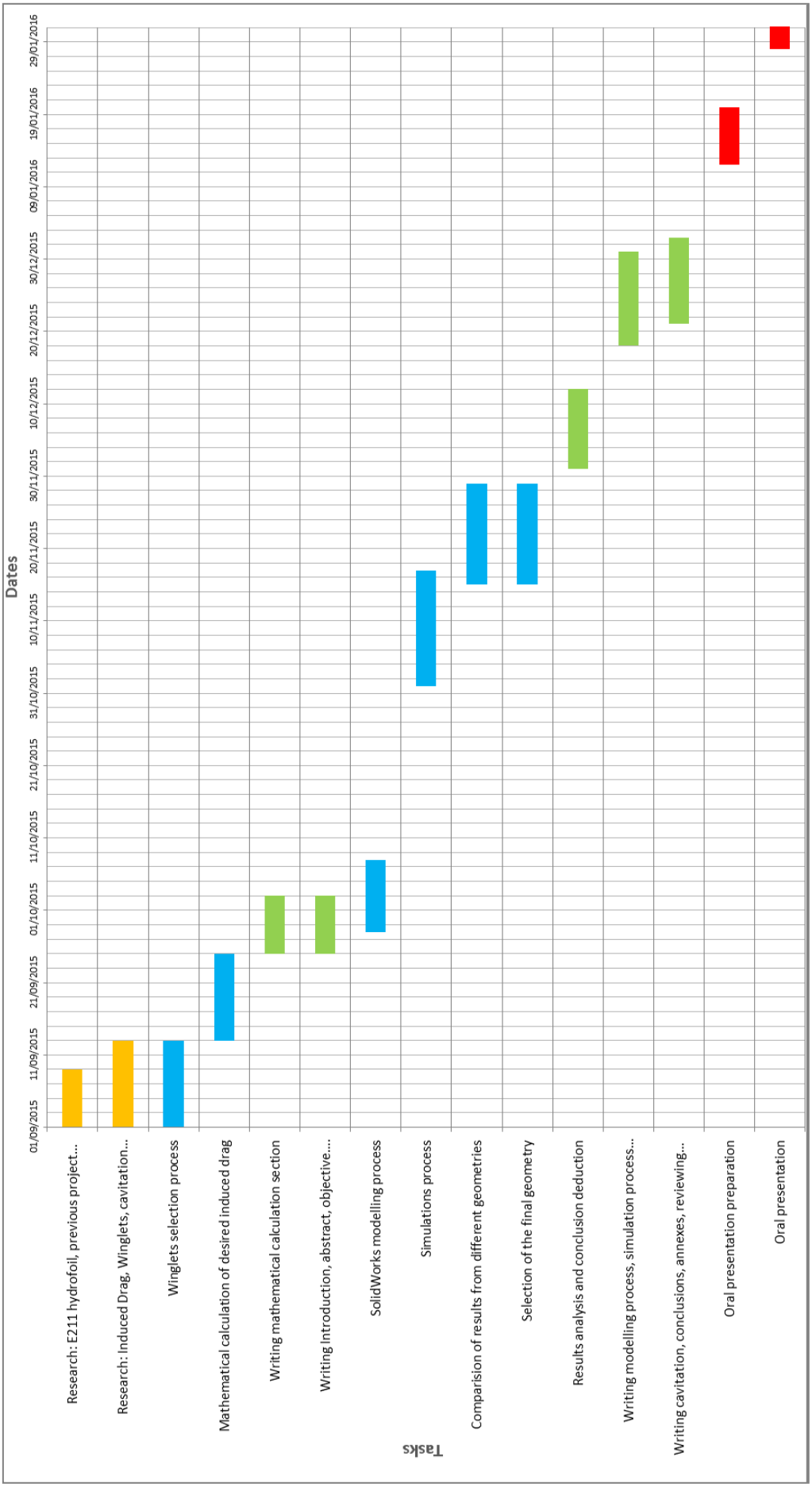

ETSEIB

Conclusion.

The main objective of this project was to analyze the effects that derive from the addition of wingtip devices to a E211 hydrofoil, in order to optimize its performance by reducing the induced drag caused by the wingtip vortices. As it can be deduced by the results stated in section 8, the final values of induced drag state a noticeable decrease of induced drag after the addition of a blended winglet; and consequently, imply a substantial increase of lift. Precisely, the growth of lift is explained by the fact that part of this lift was being used to compensate the destabilizing effect that the induced drag produced on the hydrofoil. Once the induced drag coefficient had been reduced, lift grew because it no longer was forced to counterbalance drag.

On a secondary line, this project also analyzed the possibility of the appearance of cavitation phenomena. Once having verified that the working pressure of the fluid was higher that the vapor pressure of the same fluid, it was concluded that no cavitation phenomena occured. Still, some methods to alleviate the harming effects of cavitation were presented; reaching the conclusion that spryable elastomers were the best option. Furthermore, a brief analysis of the candidate materials to build a hypothetical model of a windsurfing board and its correspondent hydrofoil concluded that, among the most common used materials – which were EPS, fiberglass and EPOXY – the latter was the most suitable option. Still, a more environmentally friendly candidate was also presented: BioFoam, which is an exclusively plant-based material.

Therefore, the general inference is that the main objective of this project was met, and that it gives rise to some amelioration that could set a new project focused on a better refinement of the obtained results, performing a severe betterment of the current winglet, building a prototype, testing it, and carrying out some further studies of new construction materials like BioFoam.

Acknowledgements.

First of all, it is essential to me to express my gratitude towards the unmeasurable help of professor and tutor of this project Enric Trillas, whose inestimable advices exerted an invigorating effect on this project and contributed to generate an endless source of hard work, which has been entirely poured into this project. His unbounded patience, limitless availability at ungodly hours of the night, and passion for teaching have been irreplaceable for me.

Furthermore, I find it impossible not to thank the infinite forbearance of my parents, whose unconditional love and good humor have helped me endure this arduous task that is not only elaborating a final degree project, but going through all these years of university studies.

Finally, I would like to thank the boundless moral support and patience of many of my really good friends, whose continuous presence has been so rewarding and tender that seems almost impossible to describe.

References.

[1] Harris, Bob, "Sailing Hydrofoils: Hydrofoils", (Hythe, Kent, England: John Morwood), December 1957.

[2] Robert V. Bruce, *Bell: Alexander Graham Bell and the conquest of Solitude*, 1st Edition, (Ithaca, United States: Cornell University Press), 2nd January 1990.

[3] Owen Dumpleton, "Sailing Hydrofoils: A Catfoil design", (Hythe, Kent, England: John Morwood), April 1956.

[4] James Grogono, *Icarus: The Boat That Flies*, 1st Edition, (Florida, United States: Sheridan House Inc.), 1st December 1987.

[5] Robert B. Harris, "Sailing Hydrofoils: Hydrofoil craft", (Hythe, Kent, England: John Morwood), June 1958.

[6] John Morwood, "Sailing Hydrofoils: The Design of Hydrofoils", (Hythe, Kent, England: John Morwood), 1958.

[7] Dr. J. M. Meyers, Dr. D. G. Fletcher, Dr. Y. Dubief, "Lift and Drag on an Airfoil", (Washington DC.: University of Washington Press).

[8] Mohsen Jahanmir, "Aircraft Drag Reduction: An Overview", Research Report, (Göteborg, Sverige: Department of Applied Mechanics, Chalmers University of Technology), 2011.

[9] Laura Voltà, Júlia Solanes, "Hidrodinàmica i Aplicació dels Hydrofoils al Windsurf", Research Report (Barcelona, Catalunya, Spain) June 2015.

[10] D. M. Bushnell, "Procedings of Mechanical Engineers Part G – Journal Aerospace

Engineering: Aircraft Drag Reduction – A review, Review Paper, (NASA Langley Research Center, Virginia, United States), 2003.

[11] I. Kroo, "Non-planar Wing Concepts for Increased Aircraft Efficiency", Lecture Series on Innovative Configurations and Advanced Concepts for Future Civil Aircraft, (Stanford University, United States), 6 – 10th June 2005.

[12] Doug McLean, "Wingtip Devices: What they do and How they do it", Article 4, Boeing Performance and Flight Operations Engineering Conference, 2005.

[13] Phillip Eisenberg, "On the Mechanisms and Prevention of Cavitation", (Washington: Navy Dept., David W. Taylor Model Basin), 1950.

[14] Ryan Sollars, Alfred D. Beitelman, "Cavitation-Resistant Coating for Hydropower Turbines", (Portland, Oregon, United States: US Army Corps of Engineers Washington, DC), June 2011.

[15] Shuji Hattori, Takamoto Itoh, "Cavitation Erosion Resistance of Plastics", (Fukui-shi, Japan: University of Fukui), May 2011.

[16] Metaline®, "Elastomeric Spray Corrosion and Repair Materials to Protect Surfaces against Wear, Erosion, Corrosion and Cavitation", (Hildeizhausen, Germany: Metaline Surface Protection GmbH), 2012.

[17] Frank M. White, *Fluid Mechanics*, 7th Edition, (New York, New York, United States: McGraw-Hill Companies Inc.), 2011.

[18] Denis Gallagher, "Surfboards: Epoxy or Fiberglass", *https://www.choice.com.au/health-and-body/diet-and-fitness/surfing-and-snowboarding/articles/epoxy-or-fibreglass-surfboards*, (Australia, 22nd July 2014).

[19] Synbra, BioFoam, "Energy requirements and CO_2 emission for polymers", *http://www.biofoam.nl/index.php?page=testje*, 2011.

[20] AHD – Windsurfing is yours, "AFS-1 concept", *http://www.ahd-boards.com/models/afs-1/*

[21] Global Surf Industries, "Surfboard Technology"; *http://www.surfindustries.com/surfboards/technology.php*

[22] Airfoil Database, "Airfoil Tools", *http://airfoiltools.com/*, 2016.

[23] Fred George, "Understanding Winglets Technology", (United States), 2005.

Complementary Reference.

Agard, "Aircraft Drag Prediction and Reduction", Agard Report No. 273, (NASA Langley, United States), 5 – 8 August 1985.

Mohammad Sodraey, "Chapter 5 Wing Design", Research Report, (New Hampshire, United States: Daniel Webster College, University Dr. Nashua), 2011.

Michael Griebel, Thomas Dornseifer, Tilman Neunhoeffer, *Numerical Simulation in Fluid Dynamics: A practical introduction*, (Philadelphia, United States: Society for Industrial and Applied Mathematics), 1998.

Hart D., Whale D., "A Review of Cavitation – Erosion Resistant Weld Surfacing Alloys for Hydroturbines", (Auckland, New Zealand), 2011.

Masamu Koika, Tsnehisa Nagayoshi, Naoki Hamamoto, "Research on Aerodynamic Drag Recduction by Vortex Generators", No. 16, (Mitsubishi Motors Technical Review), 2004.

Naval Engineers Journal, "Hydrofoils", (Capt. Robert J. Johnston, USNR), February 1985.

Robert J. Johnston, "Interantional Hydrofoil Society (IHS): A Review of the First Twenty-Five years", 14 June 1995.

M.A. Azlin, C.F. Mat Taib, S. Kasolang, F.H. Muhammad, "CDF Analysis of Winglets at Low Subsonic Flow", (London, UK: Proceedings of the Wolrd Congress on Engineering Vol. I), 6 – 8 July 2011.

F. R. Menter, M. Kuntz, R. Langty, "Ten Years of Industial Experience with the SST Turbulence Model", (Otterfing, Germany: Begell Hause, Inc.), 2003.

R. Eppler, *Airfoil design and data.* (Berlin: Springer-Verlag), 1990.

Anderson J. D., *Fundamentals of Aerodynamics*, 5th Edition, McGraw-Hill, 2010.

"Planifica't", Atenea, Available at: *http://planificat.upc.edu/*

Universitat Politècnica de Catalunya, "Language services and resources at the UPC: Writing reports and projects", *http://www.upc.edu/slt/en/academic-communication-resources/writing-reports-and-projects/writing-reports-and-project*, 2016.

ANSYS Inc., ANSYS Fluent Theory Guide 15.0 Release, (Canonsburg, PA), November 2013.

ANSYS Inc., ANSYS Fluent Modeling and Meshing Guide 15.0 Release, (Canonsburg, PA), November 2013.

ANSYS Workbench [Software, from ETSEIB, UPC]. Available at: <http://www.ansys.com/Industries/Academic>.

SolidWorks [Software, from ETSEIB, UPC]. Available at: <http://www.solidworks.es/sw/education/mechanical-engineering-student-software.htm>.

Microsoft Office Pack [Software]. Available at: <https://products.office.com/es-es/home>.